


ARTICLE

# LUBAC regulates ciliogenesis by promoting CP110 removal from the mother centriole

Xiao-Lin Shen<sup>1\*</sup>, Jin-Feng Yuan<sup>1\*</sup>, Xuan-He Qin<sup>3,4</sup>, Guang-Ping Song<sup>1</sup>, Huai-Bin Hu<sup>1</sup>, Hai-Qing Tu<sup>1</sup>, Zeng-Qing Song<sup>1</sup>, Pei-Yao Li<sup>1</sup>, Yu-Ling Xu<sup>1</sup>, Sen Li<sup>1</sup>, Xiao-Xiao Jian<sup>1</sup>, Jia-Ning Li<sup>1</sup>, Chun-Yu He<sup>1</sup>, Xi-Ping Yu<sup>1</sup>, Li-Yun Liang<sup>1</sup>, Min Wu<sup>1</sup>, Qiu-Ying Han<sup>1</sup>, Kai Wang<sup>1</sup>, Ai-Ling Li<sup>1</sup>, Tao Zhou<sup>1</sup>, Yu-Cheng Zhang<sup>1</sup>, Na Wang<sup>1</sup>, and Hui-Yan Li<sup>1,2</sup> 

**Primary cilia transduce diverse signals in embryonic development and adult tissues. Defective ciliogenesis results in a series of human disorders collectively known as ciliopathies. The CP110–CEP97 complex removal from the mother centriole is an early critical step for ciliogenesis, but the underlying mechanism for this step remains largely obscure. Here, we reveal that the linear ubiquitin chain assembly complex (LUBAC) plays an essential role in ciliogenesis by targeting the CP110–CEP97 complex. LUBAC specifically generates linear ubiquitin chains on CP110, which is required for CP110 removal from the mother centriole in ciliogenesis. We further identify that a pre-mRNA splicing factor, PRPF8, at the distal end of the mother centriole acts as the receptor of the linear ubiquitin chains to facilitate CP110 removal at the initial stage of ciliogenesis. Thus, our study reveals a direct mechanism of regulating CP110 removal in ciliogenesis and implicates the E3 ligase LUBAC as a potential therapy target of cilia-associated diseases, including ciliopathies and cancers.**

## Introduction

Many vertebrate cells possess a primary cilium, a sensory antenna-like organelle that functions in embryogenesis, tissue homeostasis, and tumorigenesis by integrating extracellular signals, such as hedgehog and Wnt signals (Capdevila et al., 2000; Corbit et al., 2008; Gerdes et al., 2009; Rohatgi et al., 2007; Singla and Reiter, 2006; Wong et al., 2009). In quiescent cells, the primary cilium emanates from the mother centriole, which constitutes the centrosome together with the daughter centriole (Kim and Dynlacht, 2013; Nigg and Raff, 2009). Primary cilia formation is a precise and well-organized process, including ciliary vesicle (CV) formation, recruitment of tau-tubulin kinase 2 (TTBK2), removal of the CP110–CEP97 complex, transition zone (TZ) assembly, and elongation of microtubule axoneme (Sanchez and Dynlacht, 2016). Defects in primary cilia lead to a set of severe diseases collectively referred to as ciliopathies, such as Bardet–Biedl syndrome (Zaghloul and Katsanis, 2009), Joubert syndrome (Valente et al., 2010), Meckel–Gruber syndrome (Valente et al., 2010; Williams et al., 2011), and polycystic kidney disease (Bergmann et al., 2018; Pazour et al., 2002).

Two proteins CP110 and CEP97 (serves as a chaperone to stabilize CP110), which localize at the distal ends of the mother and daughter centriole, are the first proteins to regulate

ciliogenesis negatively (Spektor et al., 2007). CP110, a well-known suppressor of ciliogenesis, forms a “cap” at the distal end of the mother centriole, blocking ciliary axoneme extension to switch off the cilia assembly program in vertebrate cells (Kobayashi et al., 2011; Spektor et al., 2007; Tsang et al., 2008). At the early stage of ciliogenesis, loss of CP110 on the mother centriole effectively liberates the centrosomal role of the mother centriole and promotes the conversion from mother centriole to basal body, which is subsequently constructed into primary cilium (Bettencourt-Dias and Carvalho-Santos, 2008; Spektor et al., 2007; Yadav et al., 2016). Thus, it is generally accepted that loss of CP110 on the mother centriole is a crucial event at the onset of ciliogenesis.

During ciliogenesis, both the E3 ligase complex EDD–DYRK2–DDB1<sup>VprBP</sup> and ubiquitin ligase cofactor Neurl-4 promote the degradation of CP110, therefore affecting ciliogenesis (Goncalves et al., 2021; Hossain et al., 2017; Li et al., 2012; Loukil et al., 2017). Additionally, several proteins have been identified to be involved in the regulation of CP110 removal. TTBK2 is recruited to the mother centriole to promote the selective removal of CP110 and the extension of ciliary axoneme (Goetz et al., 2012). Microtubule affinity regulating kinase 4 and Centrin2 are also

<sup>1</sup>Nanhu Laboratory, State Key Laboratory of Proteomics, National Center of Biomedical Analysis, Beijing, China; <sup>2</sup>School of Basic Medical Sciences, Fudan University, Shanghai, China; <sup>3</sup>School of Life Sciences and Technology, Tongji University, Shanghai, China; <sup>4</sup>Shanghai East Hospital, Tongji University, Shanghai, China.

\*X.-L. Shen and J.-F. Yuan contributed equally to this paper; Correspondence to Hui-Yan Li: [hyli@ncba.ac.cn](mailto:hyli@ncba.ac.cn); Na Wang: [nwang@ncba.ac.cn](mailto:nwang@ncba.ac.cn); Yu-Cheng Zhang: [yczhang@xmail.ncba.ac.cn](mailto:yczhang@xmail.ncba.ac.cn).

© 2021 Shen et al. This article is distributed under the terms of an Attribution–Noncommercial–Share Alike–No Mirror Sites license for the first six months after the publication date (see <http://www.rupress.org/terms/>). After six months it is available under a Creative Commons License (Attribution–Noncommercial–Share Alike 4.0 International license, as described at <https://creativecommons.org/licenses/by-nc-sa/4.0/>).

required for CP110–CEP97 complex removal from the mother centriole and subsequent ciliogenesis (Kuhns et al., 2013; Prosser and Morrison, 2015). The mechanism that directly triggers CP110 removal from the mother centriole, however, remains largely unclear.

The ubiquitination system regulates various physiological processes (Haglund and Dikic, 2005; Komander and Rape, 2012; Varshavsky, 2017). The linkage types of ubiquitin are determined by seven internal lysine residues (branched ubiquitin chains) or the N-terminal methionine residue of ubiquitin (linear ubiquitin chain; French et al., 2021; Kirisako et al., 2006). The K63-, K48-ubiquitin linkages have been well studied (Ikeda and Dikic, 2008; Yau and Rape, 2016). In contrast, linear ubiquitination is less well understood. The linear ubiquitin chain assembly complex (LUBAC), comprising HOIP, HOIL-1L, and SHARPIN, is the only known E3 ligase that specifically conjugates linear ubiquitin chains to substrates (Iwai et al., 2014; Kirisako et al., 2006). So far, LUBAC mainly functions in the immune response by catalyzing the linear ubiquitination of several immunological regulators, such as NEMO (Iwai et al., 2014; Tokunaga et al., 2009), IRF3 (Chattopadhyay et al., 2016), ASC (Rodgers et al., 2014), and STAT1 (Zuo et al., 2020). Additionally, our previous study reported that LUBAC regulates chromosome alignment by linearly ubiquitinating CENP-E in mitosis (Wu et al., 2019). Thus, the biological functions of linear ubiquitination remain to be further illustrated.

In this study, we report a new function of LUBAC in ciliogenesis. We found that LUBAC promotes CP110 removal from the mother centriole during ciliogenesis by specifically catalyzing the linear ubiquitination of CP110. We further demonstrated that pre-mRNA processing factor 8 (PRPF8) localizes at the distal end of the mother centriole where it acts as the receptor for the linear ubiquitin chains to promote CP110 dissociation from the mother centriole. Thus, LUBAC-catalyzed linear ubiquitin chains construct a CP110–PRPF8 complex in which PRPF8 takes CP110 away from the mother centriole to promote ciliogenesis. In conclusion, we uncovered an essential role of linear ubiquitination in ciliogenesis and revealed a direct mechanism for CP110 removal from the mother centriole.

## Results

### LUBAC is required for ciliogenesis in mammalian cells

Our research group has been working on exploring the function of primary cilia (Hu et al., 2021; Tu et al., 2018; Wang et al., 2019; Zhang et al., 2021). We transfected HeLa cells with HOIP, the core catalytic subunit of LUBAC, and found that HOIP localizes to the centrosomes in interphase cells (Fig. S1 A). We further confirmed this observation in human retinal pigment epithelial (RPE-1) cells (Fig. S1 B). Thus, we hypothesized that LUBAC could have a role in ciliogenesis. To test this hypothesis, we depleted LUBAC components from RPE-1 cells and stained these cells with the ciliary marker acetylated  $\alpha$ -tubulin (Ac-tubulin). We codepleted HOIL-1L and SHARPIN in our experiments due to their partially redundant role in LUBAC (Gerlach et al., 2011; Ikeda, 2015). Surprisingly, depletion of HOIP or codepletion of HOIL-1L and SHARPIN significantly inhibited ciliogenesis in

RPE-1 cells after 48-h serum starvation (Fig. 1, A and B; and Fig. S1 C). We further observed this phenotype in mouse inner medullary collecting duct 3 (mIMCD-3) cells (Fig. S1, D–F). Importantly, the defective ciliogenesis caused by HOIP depletion was rescued by the exogenous expression of WT HOIP but not its ligase-inactive mutant C885S (Fig. 1 C and Fig. S1 G; Lafont et al., 2018; Smit et al., 2012; Stieglitz et al., 2012). Moreover, the immunofluorescence (IF) staining of the cell proliferation marker Ki-67 revealed that depletion of HOIP or codepletion of HOIL-1L and SHARPIN did not affect the proportion of quiescent cells under the serum starvation condition (Fig. S1, H and I). This finding indicated that the defects of ciliogenesis in LUBAC-depleted cells might not be caused by the failure of cell-cycle exit. Taken together, these data suggest that LUBAC is required for ciliogenesis in mammalian cells and that its function in ciliogenesis depends on its E3 activity.

### Loss of LUBAC causes defective ciliogenesis and ciliary dysfunction in zebrafish

Zebrafish embryos with ciliary dysfunction generally manifest defective left–right asymmetry (Capdevila et al., 2000; Long et al., 2003; Stainier et al., 2017). To further investigate the ciliary function of LUBAC in vivo, we conducted a knockdown experiment in zebrafish using two different antisense morpholino oligonucleotides (MOs) against *hoip* (also known as *rnf31*), including translation-blocking morpholino (aMO) and splice-blocking morpholino (sMO). The knockdown efficiency of aMO was validated by the EGFP intensity expressed from the pCS2-UTR-*rnf31*-EGFP plasmid with aMO target sequence (Fig. S1 J). The knockdown efficiency of sMO was analyzed by sequencing and RT-PCR (Fig. S1 K). We found that the knockdown of *rnf31* in zebrafish caused developmental abnormalities. In *rnf31*-knockdown morphants, >50% of embryos displayed curved body, and 40% of embryos had pericardial edema at 48 h post-fertilization (hpf; Fig. 1, D and E). We further performed a rescue experiment by injecting the aMO-resistant form of zebrafish *rnf31* mRNA (*rnf31*-*rez*mRNA) in *rnf31*-aMO-knockdown morphants and observed that the expression of *rnf31*-*rez*mRNA rescued curved body and pericardial edema induced by *rnf31*-aMO in zebrafish (Fig. S1, L and M).

We also observed the left–right asymmetry in control or *rnf31*-knockdown morphants as revealed by whole-mount in situ hybridization. *Cmlc2*, a cardiac mesoderm marker, expresses typically at the left side in zebrafish at 26 hpf (Yelon et al., 1999). However, in *rnf31*-knockdown morphants, >35% of embryos had middle and even right-sided expression of *cmlc2* (Fig. 1, F and G). The expression of *rnf31*-*rez*mRNA in *rnf31*-aMO-knockdown morphants could markedly rescue the defects of the left–right asymmetry (Fig. S2, L and N). These data suggest that LUBAC is essential for the left–right asymmetry in zebrafish.

Since cilia in Kupffer's vesicle (KV) drive the fluid flow to control left–right asymmetry (Essner et al., 2005; Juan et al., 2018), we next detected ciliogenesis by staining Ac-tubulin in KV at the 10 somite stage. The results showed that the number of cilia in KV significantly decreased in *rnf31*-knockdown morphants (Fig. 1, H and I). Therefore, our data suggest that LUBAC is required for ciliogenesis and ciliary function in zebrafish embryos.

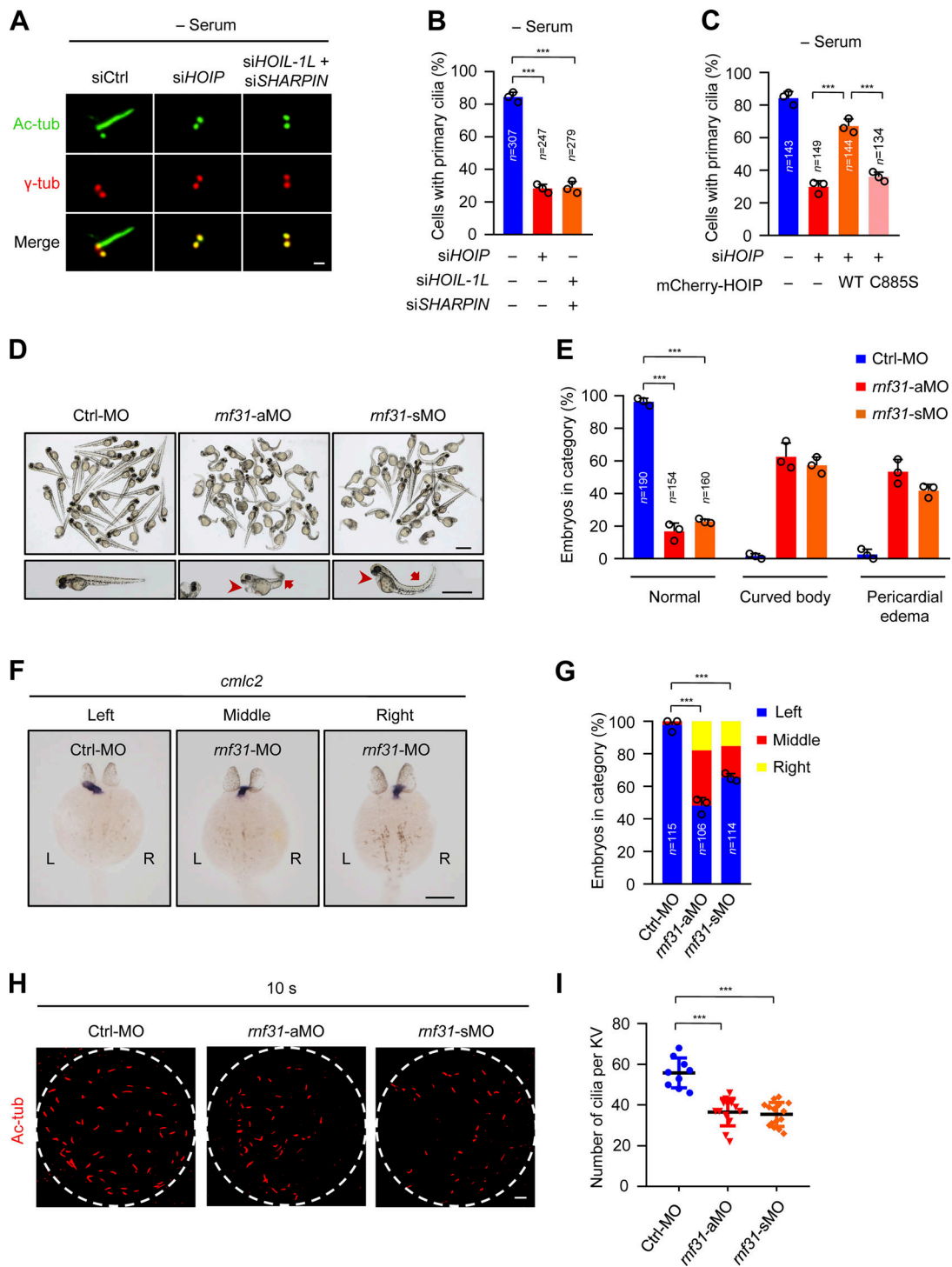


Figure 1. **The linear ubiquitin ligase complex LUBAC is required for ciliogenesis in human cells and zebrafish.** (A) RPE-1 cells were transfected with control or LUBAC component siRNAs. The cells were serum starved for 48 h and stained with the ciliary marker Ac-tubulin (Ac-tub) and  $\gamma$ -tubulin ( $\gamma$ -tub). Scale bar, 1  $\mu$ m. (B) Effects of LUBAC depletion on ciliogenesis in the absence of serum in RPE-1 cells. (C) The mCherry-tagged, RNAi-resistant form of WT HOIP, but not C885S mutant, rescued the defects of ciliogenesis in HOIP-depleted RPE-1 cells. Quantification of the ciliated cells in mCherry-positive RPE-1 cells. (D) Knockdown of *mf31* (aMO and sMO) in zebrafish caused the curved body and pericardial edema at 48 hpf. Scale bars, 1 mm. The arrows mark curved body, and arrowheads mark pericardial edema. (E) Quantification of curved body and pericardial edema in D. (F) *mf31*-knockdown morphants displayed left-right asymmetry defects. The *cmc2* probe was used to label the heart loop in the whole-mount in situ hybridization at 26 hpf. Scale bar, 200  $\mu$ m. (G) Quantification of left-right asymmetry in F. (H) Knockdown of *mf31* (aMO and sMO) impaired ciliogenesis in KV at 10 somite stage (10 s). Scale bar, 10  $\mu$ m. (I) Quantification of the cilia number of KV in H. Each dot represents one fish. Data are presented as mean  $\pm$  SD of three independent experiments in B, C, E, G, and I. \*\*\*,  $P < 0.001$  by one-way ANOVA with Dunnett's multiple comparisons test in B, E, G, and I and Bonferroni's multiple comparisons test in C. Ctrl, control.

### LUBAC specifically modulates CP110–CEP97 complex removal

To understand how LUBAC regulates ciliogenesis, we carefully examined the effect of LUBAC knockdown on the centrosome structure and various steps of ciliogenesis. Depletion of LUBAC did not disrupt the localization of  $\gamma$ -tubulin and pericentrin, suggesting that LUBAC does not affect the integrity of the centrosome (Fig. 2, A and B; and Fig. S2 A). The subdistal appendage marker ODF2 and two distal appendage proteins CEP164 and FBF1 also maintained their regular localization in LUBAC-depleted cells, indicating that LUBAC is dispensable for subdistal and distal appendage assembly (Fig. 2, A and C; and Fig. S2, B and C). Next, we tested whether depletion of LUBAC affects CV formation at the initial stage of ciliogenesis. We found that MYO5A and IFT20, which are required for CV formation (Joo et al., 2013; Wu et al., 2018), were normally localized to the ciliary base in LUBAC-depleted cells (Fig. 2, A and D; and Fig. S2 D). These data suggest that LUBAC is not responsible for CV formation.

We next detected TTBK2 recruitment and CP110–CEP97 complex removal in LUBAC-depleted cells. Interestingly, TTBK2 could be normally recruited to the mother centrioles in LUBAC-depleted cells (Fig. S2 E). However, CP110 and CEP97 were abnormally preserved on the mother centrioles when LUBAC was absent in quiescent cells (Fig. 2, E and F). These findings indicated that LUBAC is required for the removal of the CP110–CEP97 complex from the mother centriole in ciliogenesis. We also examined the localization of TZ proteins, including MKS1 (Williams et al., 2011), TMEM67 (Garcia-Gonzalo et al., 2011; Sang et al., 2011), and NPHP8 (Sang et al., 2011). LUBAC-depleted cells displayed proper localization of TZ proteins (Fig. S2, F–H).

Next, we hypothesized that LUBAC promotes ciliogenesis by directly regulating CP110–CEP97 complex removal. We then deleted CP110 in HOIP-depleted cells and found that knockdown of CP110 significantly rescued the defective ciliogenesis caused by depletion of HOIP (Fig. 2, G–I). Collectively, our data suggest that LUBAC regulates ciliogenesis by affecting the removal of the CP110–CEP97 complex on the mother centriole.

### Ciliary suppressor CP110 is a substrate of LUBAC

Considering that LUBAC specifically affects CP110–CEP97 complex removal during ciliogenesis and its E3 activity is required for ciliogenesis, we speculated that CP110 or CEP97 might be a substrate of LUBAC. We first tested whether LUBAC interacts with CP110 or CEP97 in human embryonic kidney (HEK293T) cells by ectopically expressing LUBAC. The results showed that LUBAC efficiently binds to CP110 and CEP97 (Fig. 3 A). We further confirmed that endogenous CP110 and CEP97 were present in same complex with the HOIP core catalytic subunit of LUBAC in RPE-1 cells (Fig. 3 B). Next, we investigated whether LUBAC could catalyze the linear ubiquitination of CP110 or CEP97. Interestingly, CP110, but not CEP97, could be linearly ubiquitinated by LUBAC (Fig. 3 C), as revealed by an antibody that specifically recognized linear polyubiquitin chains (Keusekotten et al., 2013; Matsumoto et al., 2012; Rivkin et al., 2013; Rodgers et al., 2014). Moreover, unlike the WT LUBAC, the ligase-inactive mutant C885S failed to linearly ubiquitinate CP110 (Fig. 3 D). Meanwhile, the linear ubiquitination of CP110

could be abrogated by coexpression of OTULIN (Fig. 3 E), which is the known linear ubiquitin-specific deubiquitinase and specifically hydrolyzes the linear ubiquitin chains of substrates (Keusekotten et al., 2013; Rivkin et al., 2013). These data suggest that CP110 might be a substrate of LUBAC.

To further validate our hypothesis, we performed an *in vitro* ubiquitination assay using His-HOIP-RBR-LDD (Fu et al., 2021; Smit et al., 2012). The results revealed that CP110 could be linearly ubiquitinated by His-HOIP-RBR-LDD (Fig. 3 F), indicating that CP110 is the substrate of LUBAC. We next investigated whether endogenous CP110 could also be linearly ubiquitinated by LUBAC during ciliogenesis. The results showed that the linear ubiquitination of endogenous CP110 could be detected in RPE-1 cells under serum starvation and that HOIP depletion substantially weakened the linear ubiquitination of CP110 (Fig. 3 G). These results indicated that LUBAC specifically mediates the linear ubiquitination of CP110 during ciliogenesis. Consistently, LUBAC and linear ubiquitin chains could localize to the centrosome in RPE-1 cells (Fig. S3, A and B). Taken together, our data suggest that CP110 is a bona fide substrate of LUBAC in ciliogenesis.

### Abrogation of the linear ubiquitination of CP110 prevents CP110 removal and ciliogenesis

To further confirm the requirement of the linear ubiquitination of CP110 in ciliogenesis, we delineated the interacting region of CP110 with HOIP. The results showed that the C-terminal region (residues 832–991) of CP110 was sufficient to interact with HOIP (Fig. 4 A; and Fig. S4, A and B). We next constructed a CP110 mutant with residues 832–991 deleted ( $\Delta$ 832–991) and performed a coimmunoprecipitation experiment. The results showed that  $\Delta$ 832–991 mutant almost lost its ability to interact with HOIP compared with WT CP110 (Fig. 4 B). This finding indicated that the residues 832–991 of CP110 are responsible for interacting with HOIP. Moreover, we found that  $\Delta$ 832–991 mutant could hardly be linearly ubiquitinated by LUBAC (Fig. 4 C). These data suggest that LUBAC catalyzes the linear ubiquitination of CP110, depending on the CP110–HOIP interaction.

Next, we generated the stable RPE-1 cell lines expressing Flag-tagged WT CP110 or  $\Delta$ 832–991 mutant and then knocked down the endogenous CP110 in these cells using siRNA against CP110. The expression level of exogenous CP110 was equal to that of the endogenous CP110 (Fig. S4 C). Strikingly, WT CP110 normally disappeared from the mother centrioles in CP110-depleted cells after serum starvation, whereas  $\Delta$ 832–991 mutant was abnormally preserved on both centrioles (Fig. 4, D and E). More importantly, compared with WT CP110, the cells expressing  $\Delta$ 832–991 mutant displayed defective ciliogenesis (Fig. 4, D and F). Thus, these data suggest that the abrogation of the linear ubiquitination of CP110 leads to the failure of its removal and defective ciliogenesis.

Since OTULIN could abrogate the linear ubiquitination of CP110 in a manner that depended on its catalytic activity (Fig. S4 D), we next detected whether OTULIN affects CP110 removal and ciliogenesis by overexpressing WT OTULIN and its ligase-dead CS mutant in RPE-1 cells. The results showed that the overexpression of WT OTULIN, but not its ligase-dead CS

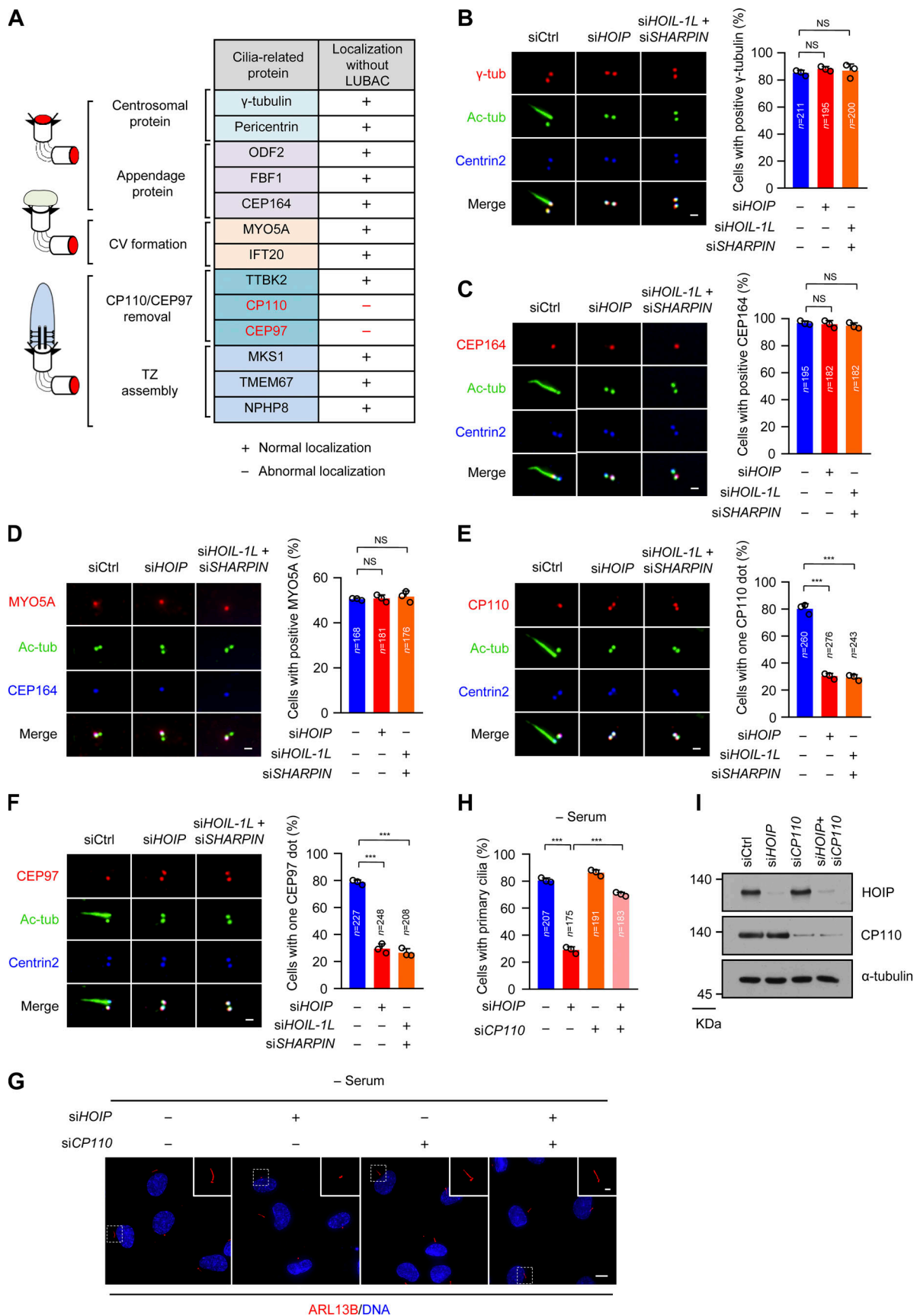


Figure 2. **Depletion of LUBAC specifically affects CP110-CEP97 complex removal during ciliogenesis.** (A) A table summarizing the centrosome localization of cilia-associated proteins in LUBAC-depleted RPE-1 cells. (B-F) RPE-1 cells were transfected with control or LUBAC component siRNAs and serum

starved for 30 min (D) or 48 h (B, C, E, and F). The cells were stained with indicated antibodies. Scale bar, 1  $\mu$ m. **(B)** The localization of centrosomal protein  $\gamma$ -tubulin ( $\gamma$ -tub) was not affected by depletion of LUBAC. **(C)** The localization of the distal end appendage marker CEP164 was not disrupted by LUBAC depletion. **(D)** MYO5A was normally localized at the mother centriole in LUBAC-depleted cells. **(E and F)** Depletion of LUBAC affected the removal of CP110 and CEP97 from the mother centrioles. **(G)** Knockdown of CP110 rescued the defective ciliogenesis in HOIP-depleted cells. RPE-1 cells were transfected with HOIP or CP110 siRNAs or cotransfected with HOIP and CP110 siRNAs. Cells then were serum starved for 48 h and stained with ARL13B (red). Insets show zoomed-in views of the boxed regions. Scale bars, 10  $\mu$ m (main image) and 2  $\mu$ m (magnified region). **(H)** Quantification of the ciliated cells in G. **(I)** Immunoblot of the RPE-1 cell lysates in G with the indicated antibodies. Data are presented as mean  $\pm$  SD of three independent experiments in B–F and H. \*\*\*,  $P < 0.001$  by one-way ANOVA with Dunnett's multiple comparisons test in B–F and Bonferroni's multiple comparisons test in H. Ctrl, control.

mutant, strongly inhibited CP110 removal and ciliogenesis under serum starvation (Fig. S4, E–H). These results further suggested that the abolishment of the linear ubiquitination of CP110 suppressed its removal and ciliogenesis. Taken together, these data suggest that linear ubiquitination of CP110 by LUBAC is required for CP110 removal and subsequent ciliogenesis.

### PRPF8 is a receptor for the linear ubiquitin chains of CP110

Next, we investigated how linear ubiquitin chains regulate CP110 removal from the mother centriole during ciliogenesis. Because linear ubiquitination mainly mediates signal transduction instead of degradation (Rahighi et al., 2009), we speculated that there might be receptors for the linear ubiquitin chains of CP110 to facilitate this process. GST pulldown experiments were conducted to enrich probable binding proteins of linear ubiquitin chains using GST-tagged linear tetraubiquitin (Ub4). The bound proteins of linear ubiquitin chains were identified by mass spectrometry (MS; Table S1). Among these candidate proteins, four have been shown to promote ciliogenesis (Fig. S5 A; Hong et al., 2015; Hossain et al., 2017; Shearer et al., 2018; Whewey et al., 2015). PRPF8 has the highest peptide coverage in four candidate proteins (Fig. S5, A and B). We thus tested the possibility that PRPF8 acts as the receptor of the linear ubiquitin chains of CP110. We first confirmed that PRPF8 could bind to GST-Ub4 (Fig. 5 A). Importantly, the linear-ubiquitinated CP110 by LUBAC, but not non-linear-ubiquitinated CP110, could efficiently bind to endogenous PRPF8 (Fig. 5 B). Collectively, these data suggest that PRPF8 acts as the receptor for the linear ubiquitin chains of CP110.

We next investigated whether the depletion of PRPF8 in RPE-1 cells causes similar effects as the knockdown of LUBAC. Strikingly, depletion of PRPF8 in RPE-1 cells dramatically suppressed CP110 removal from the mother centrioles after serum starvation and significantly inhibited ciliogenesis (Fig. 5, C–E; and Fig. S5 C). Importantly, depletion of CP110 significantly rescued the defective ciliogenesis in PRPF8-depleted cells (Fig. 5, F–H). Taken together, these data suggest that PRPF8 regulates ciliogenesis by promoting CP110 removal from the mother centriole.

### PRPF8 together with CP110 disappears from the distal end of the mother centriole in the initiation of ciliogenesis

To further confirm whether PRPF8 could act as the receptor of linear ubiquitin chains of CP110 during ciliogenesis, we detected the endogenous localization of PRPF8 in RPE-1 cells. Consistent with the previous study, PRPF8 was mainly localized in the nucleus (Fig. S6 A, control cell). Interestingly, we also found that PRPF8 localized at the mother centriole (marked by CEP164; Fig.

S6 A, control cell). Meanwhile, the IF signals of PRPF8 in the nucleus and the mother centriole were strongly reduced in PRPF8-depleted cells compared with control cells, testifying to the specificity of PRPF8 antibody (Fig. S6 A).

We further defined the localization of PRPF8 on the mother centriole using several centriolar markers, including centriole proximal end marker C-Nap1, centriole distal end marker Centrin2, subdistal appendage marker ODF2, and distal appendage marker CEP164. The results showed that PRPF8 colocalized with Centrin2 and CEP164, but not C-Nap1 or ODF2 (Fig. 6 A), suggesting that PRPF8 localized at the distal end of the mother centriole. We also observed that PRPF8 colocalized with CP110 (Fig. 6, B and C). Thus, these data indicate that PRPF8 colocalizes with CP110 at the distal end of the mother centriole.

We further detected the localization of PRPF8 on the mother centriole during ciliogenesis. Interestingly, we found that PRPF8 gradually disappeared from the distal ends of the mother centrioles at the initial stage of ciliogenesis (serum starvation 0–12 h; Fig. 6, D and F). The timing of PRPF8 loss was highly coincident with the removal of CP110 from the mother centrioles (Fig. 6, E and F). In addition, depletion of LUBAC did not affect the loss of PRPF8 on the mother centriole during ciliogenesis (Fig. 6, G and H), suggesting that the disappearance of PRPF8 from the mother centriole is independent of LUBAC. Interestingly, after serum starvation for 12 h, the percentage of ciliated cells rapidly increased, and PRPF8 localized at the ciliary base in ciliated cells (Fig. S6, B and C), which is consistent with a previous study (Whewey et al., 2015). We propose that PRPF8 first disappears from the mother centriole and then localizes to the ciliary base during ciliogenesis. Collectively, these data demonstrate that PRPF8, similar to CP110, disappears from the mother centriole at the initial stage of ciliogenesis.

### PRPF8 promotes CP110 removal to initiate ciliogenesis by binding to the linear ubiquitin chains

A previous study reported that the JAB1/MPN domain (known as ubiquitin-binding domain) of PRPF8 is sufficient to bind to K63-linked ubiquitin chains (Song et al., 2010). However, our data showed that two regions (residues 1301–1669 and 2234–2335) of PRPF8, but not the JAB1/MPN domain, could bind to the linear ubiquitin chains (Fig. 7, A and B; and Fig. S7 A). We next created a PRPF8 mutant without the linear ubiquitin-binding regions (residues 1301–1669 and 2234–2335;  $\Delta$ LUB). As expected,  $\Delta$ LUB mutant compromised its ability to bind to the linear ubiquitin chains (Fig. 7 C). Therefore, these data indicate that these two regions of PRPF8 are critical for binding to the linear ubiquitin chains.

To further confirm whether PRPF8 regulates CP110 removal and ciliogenesis through its binding to the linear ubiquitin

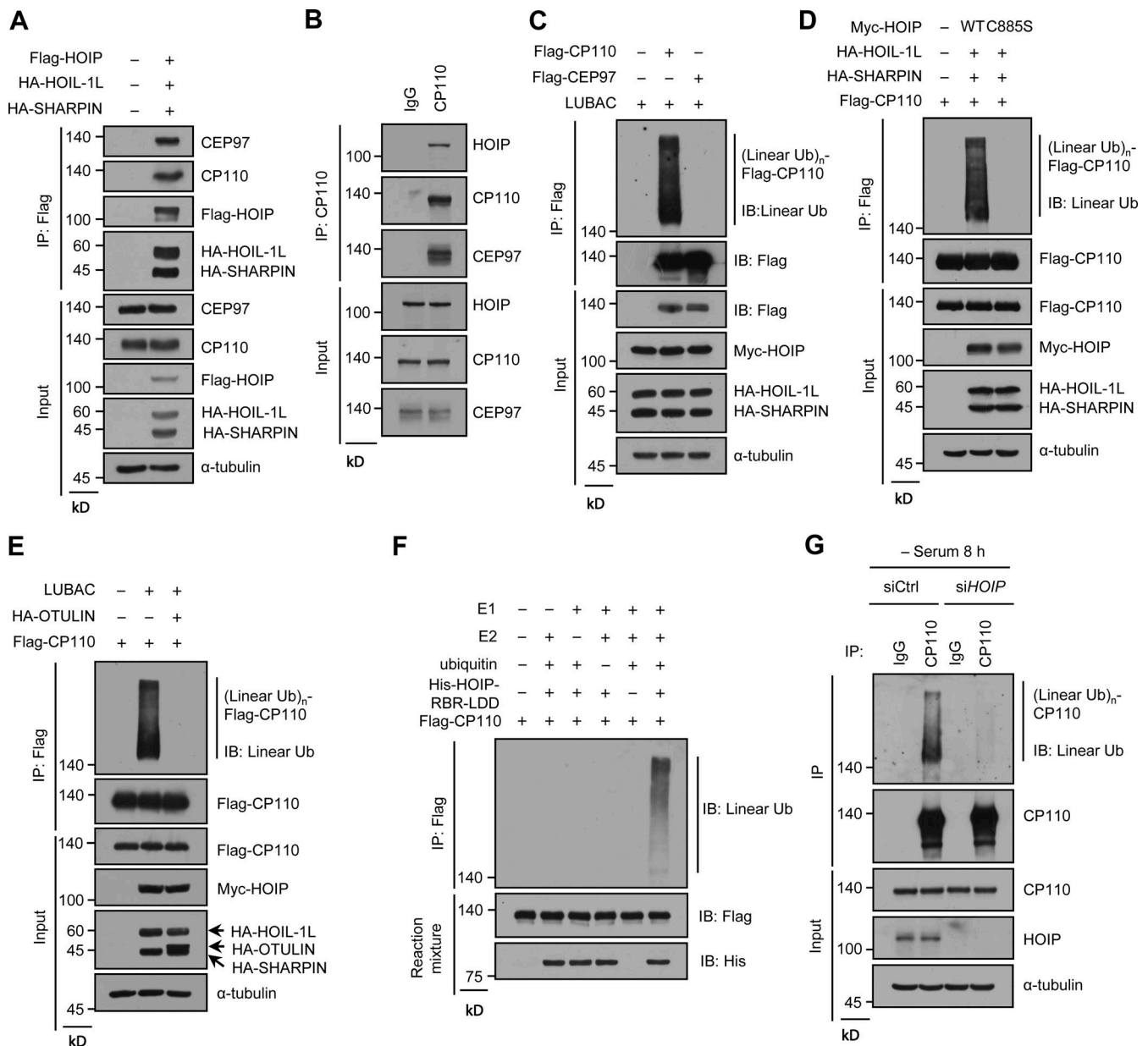


**Figure 3. LUBAC conjugates linear ubiquitin chains to CP110 during ciliogenesis.** (A) LUBAC components were transfected into HEK293T cells, and then the cell lysates were immunoprecipitated with ANTI-FLAG M2 Affinity Gel. Endogenous CP110, CEP97, and LUBAC components in immunoprecipitates and cell lysates were detected with the indicated antibodies. (B) RPE-1 cell lysates were immunoprecipitated with rabbit anti-CP110 polyclonal antibody or rabbit IgG. The immunoprecipitates and cell lysates were analyzed by immunoblotting with the indicated antibodies. (C) Linear ubiquitination assay of CP110 and CEP97. Flag-CP110 or Flag-CEP97 was transfected into HEK293T cells with or without LUBAC components. The cell lysates then were prepared according to the procedures of CP110 linear ubiquitination analysis in the Materials and methods section and immunoprecipitated with ANTI-FLAG M2 Affinity Gel. The immunoprecipitates and cell lysates were analyzed by immunoblotting with indicated antibodies. (D and E) HEK293T cells were transfected with Flag-CP110 and LUBAC WT or C885S mutant (D) or together with HA-OTULIN (E). The subsequent linear ubiquitination assay procedures were similar to C. (F) In vitro ubiquitination assay of CP110 was performed by incubating the eluted Flag-CP110 with E1, E2, His-HOIP-RBR-LDD, and ATP. The reaction mixtures were immunoprecipitated with ANTI-FLAG M2 Affinity Gel. The immunoprecipitates and reaction mixtures were analyzed by immunoblotting with indicated antibodies. (G) Linear ubiquitination assay of endogenous CP110. RPE-1 cells were treated with control or HOIP siRNAs and serum starved for 8 h. The cell lysates were immunoprecipitated with anti-CP110 polyclonal antibody or rabbit IgG, and then the immunoprecipitates and cell lysates were analyzed by immunoblotting with the indicated antibodies. IB, immunoblot; IP, immunoprecipitation; Ub, ubiquitin; (Linear Ub)<sub>n</sub>, poly-linear ubiquitin chains.

chains, we ectopically expressed WT PRPF8 or ΔLUB mutant in PRPF8-depleted RPE-1 cells. The results showed that unlike WT PRPF8, ΔLUB mutant failed to promote CP110 removal from the mother centrioles after serum starvation (Fig. 7, D and E; and Fig. S7 B). Importantly, compared with WT PRPF8, ΔLUB mutant

could not rescue the defects of ciliogenesis caused by depletion of PRPF8 (Fig. 7 F). Since the mutation (R2310K) of PRPF8 had been shown to lead to the defect of spliceosome assembly and reduce the splicing efficiency (Malinova et al., 2017; Pena et al., 2007), we next detected whether PRPF8 affects ciliogenesis

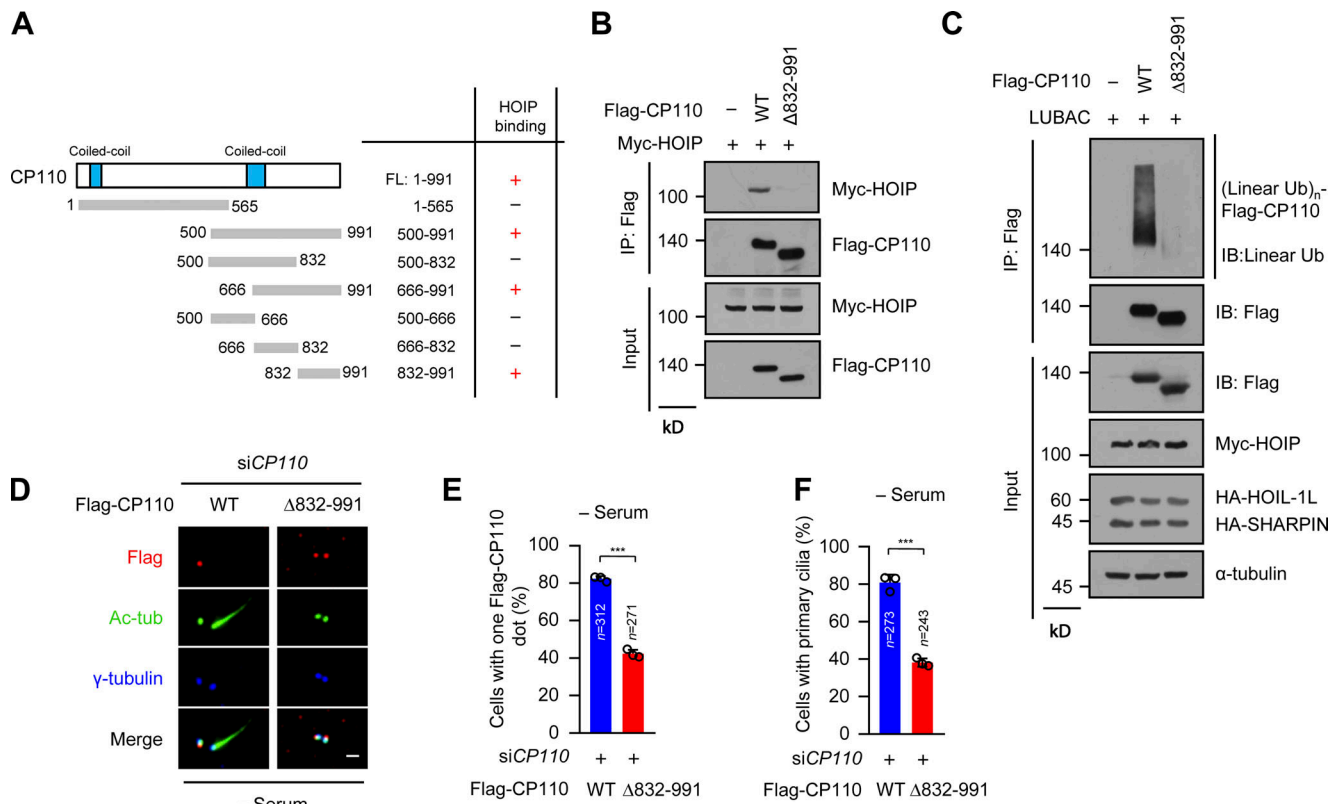


**Figure 4. A CP110 mutant unable to bind to HOIP fails to be removed from the mother centrioles and inhibits ciliogenesis. (A)** Schematic of the interaction region of CP110 with HOIP. +, interaction, -, no interaction. **(B)** The interaction of Flag-CP110 WT and Δ832-991 mutant with Myc-HOIP. HEK293T cells were transfected with Myc-HOIP together with Flag-vector (-), Flag-CP110 WT, or Δ832-991 mutant. The cell lysates were immunoprecipitated with ANTI-FLAG M2 Affinity Gel, then the immunoprecipitates and cell lysates were detected by immunoblotting with indicated antibodies. **(C)** Linear ubiquitination assay of Flag-CP110 WT and Δ832-991 mutant in HEK293T cells cotransfected with LUBAC components. **(D)** RPE-1 stable cell line expressing Flag-CP110 WT and Δ832-991 mutant were transfected with control or CP110 siRNAs and serum starved for 48 h. The cells were stained with the indicated antibodies. Scale bar, 1 μm. **(E)** Quantification of cells with one CP110 dot in Flag-positive RPE-1 cells in D. **(F)** Quantification of the ciliated cells in Flag-positive RPE-1 cells in D. Data are presented as mean ± SD of three independent experiments in E and F. \*\*\*, P < 0.001 by unpaired two-tailed t test. FL, full-length; IB, immunoblot; IP, immunoprecipitation; tub, tubulin; Ub, ubiquitin; (Linear Ub)<sub>n</sub>, poly-linear ubiquitin chains.

depending on its splicing function. The results showed that akin to WT PRPF8, PRPF8-R2310K mutant could rescue the defects of ciliogenesis induced by depletion of PRPF8 (Fig. S7, C and D), indicating that PRPF8 regulates ciliogenesis independently of its function on pre-mRNA splicing. These data suggest that PRPF8 regulates CP110 removal and further promotes ciliogenesis, depending on its ability to bind to the linear ubiquitin chains.

## Discussion

Cilia formation is strictly controlled by a set of precise biological processes (Kim and Dynlacht, 2013; Sanchez and Dynlacht, 2016). Inappropriate ciliogenesis leads to a group of diseases termed ciliopathies (Badano et al., 2006). It is well known that CP110 must be removed from the mother centriole to initiate cilia assembly when cells are exposed to cell-cycle exit signals or are serum starved (Spektor et al., 2007). Although several studies have focused on the removal of CP110 in ciliogenesis (Huang et al., 2018; Nagai et al., 2018), the molecular mechanism that directly regulates CP110 removal is still unclear. Here, we uncovered a direct mechanism for CP110 removal from the

mother centriole in ciliogenesis. In this mechanism, LUBAC directly targets CP110 and catalyzes its linear ubiquitination. Subsequently, PRPF8 at the distal end of the mother centriole interacts with the linear ubiquitin chains of CP110 and promotes the removal of CP110 from the mother centriole, thus initiating ciliogenesis (Fig. 7 G).

Previous studies have shown that the E3 ligase complex EDD-DYRK2-DDB1<sup>VPrBP</sup> promotes ciliogenesis by mediating ubiquitination and degradation of CP110 (Goncalves et al., 2021; Hossain et al., 2017). Our MS data showed that EDD (UBR5) might be a LUB candidate protein (Fig. S5 A). Based on these two reports and our data, EDD (UBR5) is possibly recruited by linear ubiquitin chains of CP110 to further facilitate the CP110 degradation after the removal of linear ubiquitinated CP110 by PRPF8 from the mother centriole.

It has been reported that LUBAC has a well-established role in immunity and is involved in angiogenesis during embryonic development (Iwai and Tokunaga, 2009; Iwai et al., 2014; Peltzer et al., 2014, 2018; Ikeda, 2015). In this study, we reveal a new and critical role of LUBAC in ciliogenesis. We found that loss of LUBAC leads to defective ciliogenesis in mammalian cells.



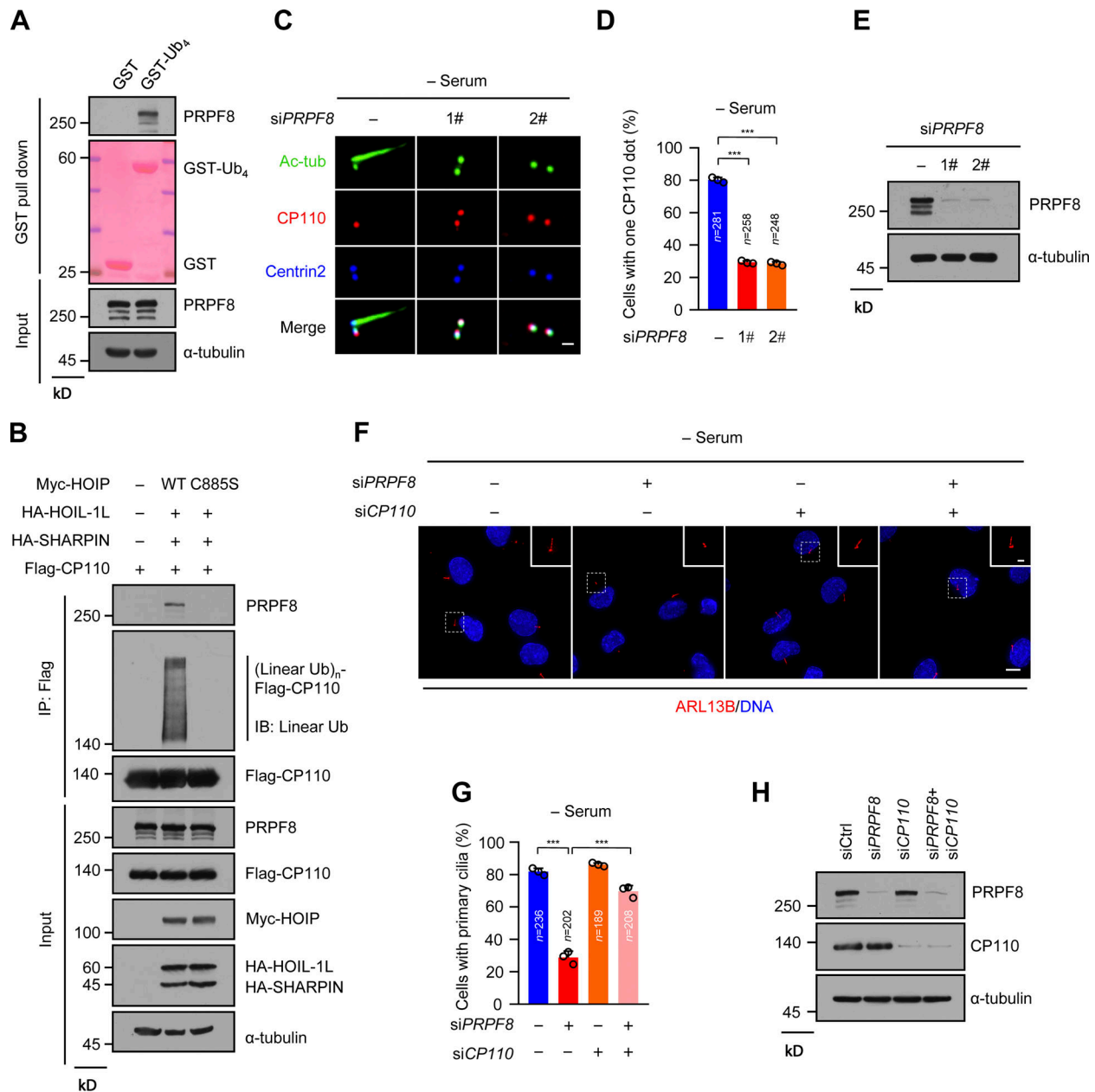


**Figure 5. PRPF8 is a receptor for the linear ubiquitin chains of CP110 and promotes CP110 removal during ciliogenesis. (A)** RPE-1 cells were serum starved for 8 h, then the cell lysates were pulled down by GST or GST-Ub<sub>4</sub>, with GST as a negative control. Endogenous PRPF8 was detected by anti-PRPF8 antibody. GST and GST-Ub<sub>4</sub> were stained by Ponceau S. **(B)** Flag-CP110 was transfected into HEK293T cells with or without LUBAC WT or C885S mutant. The cell lysates were immunoprecipitated with ANTI-FLAG M2 Affinity Gel, and then the immunoprecipitates and cell lysates were analyzed by immunoblotting with the indicated antibodies. **(C)** RPE-1 cells were transfected with control or two individual *PRPF8* siRNAs followed by serum starvation for 48 h. The cells were stained with the indicated antibodies. Scale bars, 1 μm. **(D)** Quantification of cells with one CP110 dot in RPE-1 cells in C. **(E)** Immunoblot of the RPE-1 cell lysates in C with the indicated antibodies. **(F)** Knockdown of CP110 rescued the defective ciliogenesis in *PRPF8*-depleted cells. RPE-1 cells were transfected with *PRPF8* or *CP110* siRNAs or cotransfected with *PRPF8* and *CP110* siRNAs. Cells then were serum starved for 48 h and stained with ARL13B (red). Insets show zoomed-in views of the boxed regions. Scale bars, 10 μm (main image) and 2 μm (magnified region). **(G)** Quantification of the ciliated cells in F. **(H)** Immunoblot of the RPE-1 cell lysates in F with the indicated antibodies. Data are presented as mean ± SD of three independent experiments in D and G. \*\*\*, *P* < 0.001 by one-way ANOVA with Dunnett’s multiple comparisons test in D and Bonferroni’s multiple comparisons test in G. Ctrl, control; IB, immunoblot; IP, immunoprecipitation; tub, tubulin; Ub, ubiquitin; (Linear Ub)<sub>n</sub>, poly-linear ubiquitin chains.

Although there is no evidence that human beings with LUBAC deficiency suffer from ciliopathies, our study might provide a clue for this issue, which should be considered in future research. In addition, because HOIP or HOIL-1L knockout mice die at embryonic day 10.5 (Peltzer et al., 2014, 2018), which vastly

limits our ability to observe cilia defects and cilia-related disease phenotypes, we chose zebrafish to study the ciliary function of LUBAC in vivo. *Rnf31*-knockdown zebrafish displayed ciliopathy-related phenotypes, such as defective left-right asymmetry (the randomized laterality of heart looping, marked by *cmlc2*).

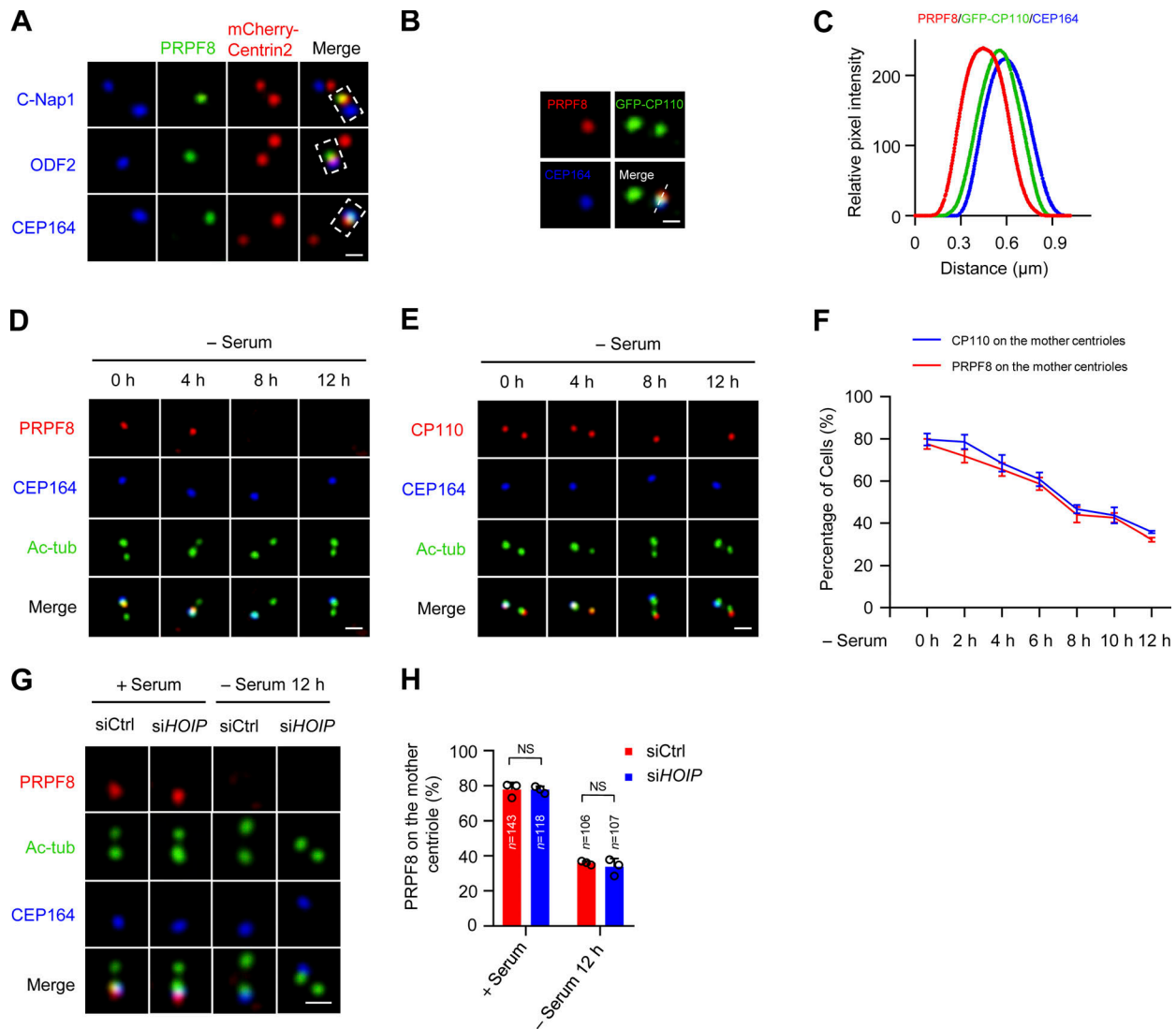


**Figure 6. PRPF8 colocalizes with CP110 and disappears from the distal end of the mother centriole in the initiation of ciliogenesis. (A)** RPE-1 cells were transfected with mCherry-Centrin2 for 24 h. The cells were stained with the indicated antibodies. PRPF8 was visualized with centriolar proximal (C-Nap1), distal (Centrin2), subdistal appendage (ODF2), and distal appendage (CEP164) markers. Scale bar, 0.5  $\mu$ m. **(B)** PRPF8 was colocalized with CP110. RPE-1 cells were transfected with GFP-CP110 for 24 h. The cells were stained with the indicated antibodies. Scale bar, 0.5  $\mu$ m. **(C)** The relation between the relative position and fluorescence intensity of PRPF8, CP110, and CEP164 in B. **(D and E)** RPE-1 cells were serum starved for the indicated time points and stained with the indicated antibodies. Scale bars, 1  $\mu$ m. Immunostaining of PRPF8 and CP110 are shown in D and E, respectively. **(F)** Line graph showing the percentages of cells with PRPF8 and CP110 on the mother centrioles in D and E. **(G)** RPE-1 cells were transfected with control or HOIP siRNAs and serum starved for the indicated time points. The cells were collected and stained with the indicated antibodies. Scale bar, 1  $\mu$ m. **(H)** Quantification of cells with centriolar PRPF8 in G. Data are presented as mean  $\pm$  SD of three independent experiments. Ctrl, control.

Therefore, we propose that LUBAC-dependent ciliogenesis might be required for embryogenesis in mammals.

Previous studies showed that PRPF8, as a scaffold protein of the spliceosome in the nucleus, participates in pre-mRNA splicing processes (Brown and Beggs, 1992; Grainger and Beggs, 2005). We found that PRPF8 localizes at the distal end of the mother centriole and plays an essential role in CP110 removal during ciliogenesis. At the beginning of ciliogenesis, PRPF8 serves as the receptor for linear ubiquitin chains of CP110 and disappears from the mother centriole to promote CP110 removal. Our results also showed that the localization and disappearance of PRPF8 on the mother centriole are independent of

LUBAC, suggesting that additional mechanisms regulate the recruitment and removal of PRPF8 on the mother centriole. Future studies are needed to clarify these mechanisms, which will be helpful to further understand the functional significance of PRPF8 in the regulation of ciliogenesis. We also observed that PRPF8 returns to the ciliary base after cilia assembly, which indicates that PRPF8 might have another function in primary cilia. This issue is valuable and worth exploring in the future.

We also identified two LUB regions (residues 1301–1669 and 2234–2335) on PRPF8. The PRPF8 mutant without these two LUB regions ( $\Delta$ LUB) failed to promote CP110 removal from the mother centrioles and could not rescue the defects of ciliogenesis

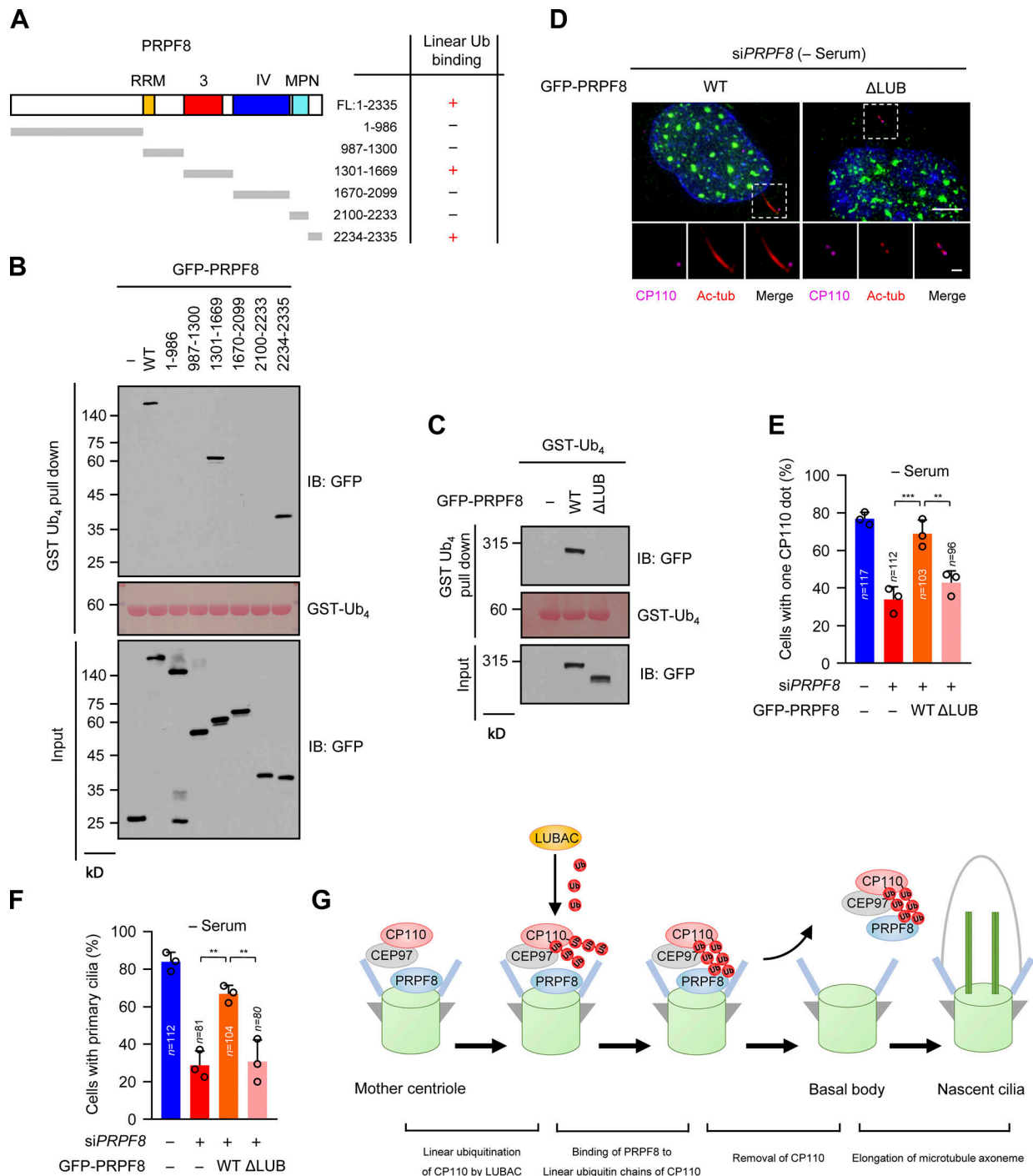


**Figure 7. PRPF8 regulates CP110 removal to promote ciliogenesis dependent on its ability to bind to the linear ubiquitin chains. (A)** Schematic representation of the regions of PRPF8 binding to the linear ubiquitin chains (GST-Ub<sub>4</sub>). +, interaction; -, no interaction. **(B)** Map of the regions of PRPF8 binding to the linear ubiquitin chains (GST-Ub<sub>4</sub>). HEK293T cells were transfected with GFP-vector, or GFP-PRPF8 truncations. The cell lysates were pulled down by GST-Ub<sub>4</sub>, and then GFP proteins were detected by anti-GFP antibody. GST-Ub<sub>4</sub> was stained by Ponceau S. **(C)** GFP-vector (-), GFP-PRPF8 WT, or ΔLUB (double depletions of residues 1301–1669 and 2234–2335 in full-length PRPF8) mutant were transfected into HEK293T cells. The subsequent GST pull-down assay procedures were similar to B. **(D)** GFP-vector (-), GFP-PRPF8 WT, or ΔLUB mutant were transfected into control or PRPF8-depleted RPE-1 cells. The cells were serum starved for 48 h and then stained with the indicated antibodies. Insets show zoomed-in views of the boxed regions. Scale bars, 5 μm (main image) and 1 μm (magnified region). **(E)** Quantification of cells with one CP110 dot in GFP-positive RPE-1 cells in D. **(F)** Quantification of the ciliated cells in GFP-positive RPE-1 cells in D. **(G)** The model of LUBAC regulating ciliogenesis. LUBAC specifically catalyzes the linear ubiquitination of the ciliary suppressor CP110. Subsequently, PRPF8 at the distal end of the mother centriole binds to the linear ubiquitin chains and facilitates the removal of the CP110–CEP97 complex from the mother centriole, therefore initiating ciliogenesis. Data are presented as mean ± SD of three independent experiments in E and F. \*\*, P < 0.01; \*\*\*, P < 0.001 by one-way ANOVA with Bonferroni's multiple comparisons test. FL, full-length; IB, immunoblot; tub, tubulin; Ub, ubiquitin.

in PRPF8-depleted cells. Although residues 2234–2335 of PRPF8 are related to its pre-mRNA splicing function, our data showed that the regulation of PRPF8 in ciliogenesis does not depend on its function on pre-mRNA splicing (Fig. S7, C and D). Of course, we cannot exclude the existence of additional deficiency on  $\Delta$ LUB mutant. Taken together, our data indicate that the critical role of PRPF8 in ciliogenesis depends on its binding to the linearly ubiquitinated CP110, although other possible mechanisms cannot be completely ruled out.

It has been reported that PRPF8 closely links to a genetic retinal degeneration called retinitis pigmentosa (RP), which is commonly considered as a ciliopathy (Farkas et al., 2014; McKie et al., 2001; Pena et al., 2007). Based on our findings, we speculate that cilia defect caused by PRPF8 dysfunction may contribute to the development of RP. Thus, our study provides an insight into the pathogenesis of RP.

In summary, our study establishes a LUBAC-mediated signaling cascade complex that promotes ciliogenesis and provides a direct explanation of how CP110 disappears from the mother centriole during ciliogenesis. Our findings also have profound implications for ciliopathy therapies. As an E3 ligase, LUBAC may be a potential treatment drug target for cilia-associated diseases, such as cancers and ciliopathies.

## Materials and methods

### Cell culture

Human RPE-1 cells and mIMCD-3 cells were a gift from Xueliang Zhu (Shanghai Institute of Biochemistry and Cell Biology, Shanghai, China). RPE-1 cells were cultured in advanced DMEM/F-12 (1:1) medium supplemented with 10% FBS, 0.01 mg/ml hygromycin B, and 1% penicillin/streptomycin. mIMCD-3 cells were cultured in advanced DMEM/F-12 (1:1) medium supplemented with 10% FBS and 1% penicillin/streptomycin. For cilia formation, RPE-1 cells or mIMCD-3 cells were starved in Opti-MEM reduced serum media (Thermo Fisher Scientific) for 48 h. HeLa cells and HEK293T cells were obtained from ATCC and grown in DMEM supplemented with 10% FBS and 1% penicillin/streptomycin. All cell lines were cultured at 37°C with 5% CO<sub>2</sub>.

### Cloning and plasmids

Myc-HOIP and HA-HOIL-1L were a gift by Dr. Kazuhiro Iwai (Kyoto University, Kyoto, Japan). HA-OTULIN was provided by Dr. Mads Gyrd-Hansen (Ludwig Institute for Cancer Research, Oxford, UK). GST-Ub4 was obtained from Dr. Ivan Dikic (Goethe University Frankfurt, Frankfurt, Germany). GFP-CP110, Flag-CP110, and Flag-CEP97 were supplied by Dr. Brian David Dynlacht (New York University Cancer Institute, New York, NY). mCherry-HOIP, mCherry-OTULIN, and mCherry-Centrin2 were amplified by PCR and cloned into the p-mCherry-C1-vector. Flag-HOIP, GFP-HOIP, HA-SHARPIN, all fragments of Flag-CP110, and  $\Delta$ 832–991 mutant were amplified by PCR and cloned into pcDNA3.0, EGFP-N1, pXJ40, or pCBF-vector. Flag-CP110 WT and  $\Delta$ 832–991 mutant stably expressed in RPE-1 cells were subcloned into pCDH-MCS-T2A-puro-MSCV-vector. GFP-PRPF8,  $\Delta$ LUB, and GFP-PRPF8 truncations were amplified by PCR and cloned into pcDNA5/FRT/TO. Myc-HOIP C885S,

mCherry-HOIP C885S, mCherry-OTULIN C129S, GFP-PRPF8 R2310K, and all siRNA-resistant plasmids were generated by PCR-based site-directed mutagenesis. All constructs were verified by sequencing. Plasmid transfection into RPE-1 cells was performed using Lipofectamine LTX Reagent (Thermo Fisher Scientific) according to the manufacturer's instructions.

### RNAi

Synthetic siRNA oligonucleotides were obtained from Thermo Fisher Scientific or Sigma-Aldrich. Transfection of siRNAs using RNAiMAX (Thermo Fisher Scientific) was performed according to the manufacturer's instructions. The sequences of siRNAs are as follows: control siRNA, 5'-UUCUCCGAACGUGUCACGUA-3'; HOIP siRNA, 5'-CACACCCUCGAGACUGCCUCUUCU-3'; HOIL-1L siRNA, 5'-CCGCUGCAGGGUAAAUGGGAUUCCU-3'; SHARPIN siRNA, 5'-UGCCUGAGCGCAGCCUUGCCUCUUA-3'; Hoip siRNA, 5'-GGACAGAGUAUUGCCCGCAGAAGAA-3'; Hoil-1l siRNA, 5'-GGAGACCUUGCAUUCACACGGCAUU-3'; Sharpin siRNA, 5'-CGCAGCCGCGGAAGCUGCAAUUGAT-3'; CP110 siRNA, 5'-GCGGCCAAAUGUUGCGACAAUUUAA-3'; PRPF8 siRNA-1#, 5'-GGAUUAUGAUGCGCCGAGA-3'; and PRPF8 siRNA-2#, 5'-CCCUCUGUCUGUGCUUGUG-3'.

### Antibodies

The antibodies used in this study included mouse anti- $\alpha$ -tubulin (1:1,000, T6793; Sigma-Aldrich), rabbit anti- $\gamma$ -tubulin (1:400, T3559; Sigma-Aldrich), rabbit anti-ARL13B (1:1,000, 17711-1-AP; Proteintech), mouse anti-Centrin2 (1:400, 04-1624; Millipore), rabbit anti-Ki-67 (1:1,000, D3B5; Cell Signaling Technology), rabbit anti-CEP164 (1:600, 45330002; Novus Biologicals), mouse anti-CEP164 (1:100, sc-515403; Santa Cruz Biotechnology), rabbit anti-pericentrin (1:400, ab4448; Abcam), rabbit anti-ODF2 (1:500, 12058-1-AP; Proteintech), mouse anti-Odf2 (1:100, sc-393881; Santa Cruz Biotechnology), rabbit anti-CP110 (IF 1:500, Western blot [WB] 1:1,000, 12780-1-AP; Proteintech), rabbit anti-mCherry (1:1,000, ab167453; Abcam), rabbit anti-CEP97 (IF 1:100, WB 1:500, 22050-1-AP; Proteintech), rabbit anti-MKS1 (1:100, 16206-1-AP; Proteintech), rabbit anti-TMEM67 (1:100, 13975-1-AP; Proteintech), rabbit anti-RPGRIPL1 (1:100, HPA039405; Sigma-Aldrich), rabbit anti-FBF1 (1:200, HPA023677; Sigma-Aldrich), rabbit anti-TTBK2 (1:500, HPA018113; Sigma-Aldrich), mouse anti-Flag (IF 1:1,000, WB 1:5,000, F3165; Sigma-Aldrich), anti-DDDDK-tag pAb-HRP-DirecT (1:1,000, PM020-7; Medical & Biological Laboratories), rabbit anti-PRPF8 (IF 1:200, WB 1:1,000, sc-030207; Santa Cruz Biotechnology), rabbit anti-PRPF8 (WB 1:1,000, ab87433; Abcam), rabbit anti-myosin-Va (IF 1:500, NBPI-92156; Novus Biologicals), mouse anti-C-Nap1 (1:100, sc-390540; Santa Cruz Biotechnology), mouse anti- $\alpha$ -tubulin (1:1,000, T5168; Sigma-Aldrich), mouse anti-Myc (1:500, sc-40; Santa Cruz Biotechnology), mouse anti-HA (1:1,000, sc-7392; Santa Cruz Biotechnology), mouse anti-GFP (1:500, sc-9996; Santa Cruz Biotechnology), sheep anti-HOIP and anti-HOIL-1L (Emmerich et al., 2013; 1:5,000; a gift from Dr. Philip Cohen, University of Dundee, Dundee, UK), rabbit anti-SHARPIN (1:1,000, #4444; Cell Signaling Technology), anti-linear ubiquitin (Matsumoto et al., 2012; IF 1:5,000, WB 1:2,500; a gift from Dr. Vishva M. Dixit, Genentech Inc., South San

Francisco, CA), rabbit anti-SHARPIN (1:500, ABF128; Millipore), and mouse anti-HOIL-IL (1:1,000, MABC576; Millipore). Rabbit anti-HOIP antibodies were produced in rabbits using a peptide containing N-terminal 203 aa of HOIP by GenScript.

## IF

To detect primary cilia and centrosome proteins, cells were placed on ice for 10 min and then fixed and permeabilized in cold methanol ( $-20^{\circ}\text{C}$ ) for 10 min. Cells transfected with plasmids were fixed in 4% PFA at  $37^{\circ}\text{C}$  for 3 min and cold methanol ( $-20^{\circ}\text{C}$ ) for 20 min. Cells were blocked with 3% normal goat serum in 0.1% Triton X-100/PBS for 1 h before incubating with primary antibodies. Secondary antibodies, including Alexa Fluor 488-, 546-, and 647-conjugated goat anti-mouse, anti-rabbit, or anti-human IgG (1:400; Thermo Fisher Scientific) were used. DNA was stained with Hoechst 33342 (1:1,000, H3570; Thermo Fisher Scientific).

For detecting cilia in KV of zebrafish, embryos were fixed in 4% PFA at room temperature overnight and blocked with 2% BSA and 0.5% normal goat serum in 1% DMSO, 0.5% Triton X-100/PBS. Anti-Ac-tubulin antibody (T6793; Sigma-Aldrich) was used to label cilia.

To use two different primary antibodies from the same species (Fig. 2, B–F; Fig. 4 D; Fig. 5 C; Fig. 6, D, E, and G; Fig. S3; and Fig. S6 A), an anti-Ac-tubulin antibody was labeled as a fluorophore using APEX Alexa Fluor 488 Antibody Labeling Kit (Thermo Fisher Scientific). After finishing the standard indirect IF procedure, cells were incubated with the labeled anti-Ac-tubulin at room temperature for 2 h.

Images were acquired at room temperature with a  $60\times/1.42$  NA oil objective (Fig. 1 A; Fig. 2, B–G; Fig. 4 D; Fig. 5, C and F; Fig. 6, A, B, D, E, and G; Fig. 7 D; Fig. S1, A, B, D, and H; Fig. S2; Fig. S3; Fig. S4 E; Fig. S6, A and B; and Fig. S7 C) on a DeltaVision Image Restoration Microscope (with an sCMOS edge 5.5 camera) or a  $40\times/0.75$  NA objective on a Zeiss LSM 880 microscope (Fig. 1 H). All acquisition settings were kept constant for experimental and control groups in the same experiment. The representative images acquired by the DeltaVision system were processed by iterative constrained deconvolution (softWoRx; Applied Precision). All raw images were analyzed with Volocity 6.0 software (PerkinElmer).

## WB

All protein samples were separated by SDS-PAGE; then, target proteins were transferred to polyvinylidene fluoride membranes and analyzed by immunoblotting using the indicated antibodies. Protein bands were visualized on x-ray film by chemiluminescence according to the manufacturer's instructions.

## Generation of stable cell lines

The stable cell lines expressing Flag-CP110 WT and  $\Delta 832-991$  mutant were generated by the following procedures: Flag-CP110 WT and  $\Delta 832-991$  mutant were cloned into pCDH-MCS-T2A-puro-MSCV-vector. Vesicular stomatitis virus G protein pseudotyped retrovector system was used for *in vivo* gene delivery, then the RPE-1 cells expressing Flag-CP110 WT or  $\Delta 832-991$

mutant were screened with  $20\ \mu\text{g}/\text{ml}$  puromycin. Subsequently, a single clone of the cells was chosen and grown in advanced DMEM/F12 (1:1) medium for WB and IF staining.

## MS analysis

To identify GST-Ub4 binding proteins, HEK293T cells were serum starved for 8 h and lysed with pull down (PD) buffer (50 mM Tris-HCl, pH 7.5, 150 mM NaCl, 1 mM DTT, 0.1% NP-40) containing complete protease inhibitor cocktail (04693132001; Roche), then cell lysates were pulled down by GST-Ub4. The immunoprecipitates were separated by SDS-PAGE and stained with Bio-Safe Coomassie (Bio-Rad). Full bands were cut down and digested with trypsin. Liquid chromatography–tandem MS (LC-MS/MS) was used to identify GST-Ub4 binding proteins. MS analysis was performed on an Orbitrap Fusion Lumos Tribrid mass spectrometer (Thermo Fisher Scientific) coupled with an EASY-nLC 1000 nanoflow LC system (Thermo Fisher Scientific).

## Immunoprecipitation

The indicated plasmids were induced into HEK293T cells with VigoFect (Vigorous Biotechnology) for 24 h. Cells were washed three times with PBS and lysed in M2 buffer (50 mM Tris-HCl, pH 7.5, 1% NP-40, 150 mM NaCl, 0.5 mM EGTA, 0.5 mM EDTA, 1 mM DTT, 1.5 mM  $\text{MgCl}_2$ , 1 mM PMSF) containing complete protease inhibitor cocktail at  $4^{\circ}\text{C}$  for 30 min. The cell lysates were centrifuged at  $15,000\ g$  at  $4^{\circ}\text{C}$  for 10 min. The lysate supernatants were incubated with ANTI-FLAG M2 Affinity Gel (A2220; Sigma-Aldrich) at  $4^{\circ}\text{C}$  for 4 h. The immunoprecipitates were washed six times with M2 buffer and resuspended in SDS sample buffer to boil at  $95^{\circ}\text{C}$  for 10 min. The immunoprecipitated proteins and cell lysates then were analyzed by immunoblotting with the indicated antibodies.

To detect the interaction between CP110–CEP97 complex and LUBAC in RPE-1 cells, RPE-1 cells were collected and lysed in M2 buffer containing complete protease inhibitor cocktail. The lysates were incubated with rabbit anti-CP110 polyclonal antibody (12780-1-AP; Proteintech) or rabbit IgG antibody (B900610; Proteintech) at  $4^{\circ}\text{C}$  overnight, then Protein A Sepharose (17-1279-01; GE Healthcare) was added and incubated at  $4^{\circ}\text{C}$  for 4 h. The immunoprecipitates were analyzed by immunoblotting with the indicated antibodies.

## Linear ubiquitin chains binding assay

GST and GST-Ub4 were purified from *Escherichia coli* using Glutathione Sepharose 4B (17-0756-01; GE Healthcare) according to the manufacturer's instructions. For GST-Ub4 and endogenous PRPF8 binding assay, RPE-1 cells were serum starved for 8 h and lysed with PD buffer containing complete protease inhibitor cocktail. The cell lysates were incubated with GST or GST-Ub4 at  $4^{\circ}\text{C}$  overnight. For the mapping PRPF8 experiments, GFP-PRPF8 WT,  $\Delta\text{LUB}$ , and all GFP-PRPF8 truncations were transiently transfected into HEK393T cells to express for 24 h. The cell lysates were prepared by lysing cells in PD buffer containing complete protease inhibitor cocktail and incubated with GST-Ub4. All GST or GST-Ub4 immunoprecipitates were detected by immunoblotting with the indicated antibodies.

### Analysis of CP110 linear ubiquitination

Flag-CP110 or Flag-CEP97 was transiently introduced into HEK293T cells with or without Myc-HOIP, HA-HOIL-1L, and HA-SHARPIN. At 24 h after transfection, cells were lysed with radioimmunoprecipitation assay (RIPA) buffer (20 mM Tris HCl, pH 7.5, 150 mM NaCl, 10 mM EDTA, 1% Triton X-100, 1% deoxycholate) containing complete protease inhibitor cocktail and N-ethylmaleimide (E3876; Sigma-Aldrich). The cell lysates were ultrasonicated and centrifuged at 15,000 *g* at 4°C for 15 min. SDS was added into the lysate supernatants (the final concentration of SDS was 1%), followed by heating at 90°C for 5 min to remove noncovalently bound proteins. The lysate supernatants then were diluted to 0.1% SDS with RIPA buffer and immunoprecipitated by ANTI-FLAG M2 Affinity Gel. The immunoprecipitates and cell lysates were analyzed by immunoblotting with the indicated antibodies. For linear ubiquitination analysis of Δ832–991 mutant, the procedures were the same.

For detecting linear ubiquitination of endogenous CP110, RPE-1 cells were transfected with control or HOIP siRNAs for 48 h. Cells were serum starved for 8 h and then lysed as described above without adding SDS and the heating procedure. The cell lysates were centrifuged at 15,000 *g* at 4°C for 15 min. The lysate supernatants were incubated with rabbit anti-CP110 polyclonal antibody (12780-1-AP; Proteintech) or rabbit IgG antibody (B900610; Proteintech) at 4°C overnight, then Protein A Sepharose was added and incubated at 4°C for 4 h. The immunoprecipitates were washed and boiled, then analyzed by immunoblotting.

### In vitro ubiquitination assay

To obtain purified CP110 proteins, Flag-CP110 was transfected into HEK293T cells for expression for 48 h, and the cells were lysed in RIPA buffer containing complete protease inhibitor cocktail at 4°C for 30 min. The cell lysates were ultrasonicated and immunoprecipitated with ANTI-FLAG M2 Affinity Gel. Next, the immunoprecipitates were washed three times with elution buffer (50 mM Tris-HCl, pH7.5, 150 mM NaCl) containing complete protease inhibitor cocktail and then eluted by 3× Flag peptides (concentration at 200 ng/μl) in elution buffer for 2 h at 4°C. The eluates were concentrated to 50 μl by Amicon Ultra Centrifugal Filters for further use.

For in vitro ubiquitination assay of CP110, the eluted Flag-CP110 was incubated at 37°C for 2 h with recombinant human His6-MBP-HOIP-RBR-LDD (E3-240-100; Boston Biochem) in Ubiquitin Conjugation Reaction Buffer (SK-10; Boston Biochem) supplemented with 100 nM UBE1 (E-305-025; Boston Biochem), 15 μM Recombinant Human Ubiquitin (U-100H; Boston Biochem), 600 nM UBE2D3 (E2-627; Boston Biochem), and 10 mM Mg-ATP. The reaction mixtures were immunoprecipitated with ANTI-FLAG M2 Affinity Gel. The immunoprecipitates were detected by immunoblotting with anti-linear ubiquitin antibodies.

### Zebrafish

All WT AB strain embryos in this study were acquired by natural spawning of adult zebrafish. The adult zebrafish were maintained in 28.5°C system water. The MOs against *rnf31* were obtained from GeneTools; the antisense sequences of MOs used are

as follows: *rnf31*-sMO, 5'-GCTGAACATGATGATTTTACCTGTT-3'; *rnf31*-aMO, 5'-ATCAGTGAGAGAGGCCATAGCGC-3'; and control-MO, 5'-CCTCTTACCTCAGTT-3'. These MOs were injected into embryos at the one-cell stage. The genotyping primers for sMO knockdown embryos are as follows: sMO-F, 5'-GTACTTAACCTGTACGGCTACACC-3', and sMO-R, 5'-TTTACACTGCCACTCAGATATTGT-3'. The RT-PCR primers for sMO knockdown embryos are as follows: E5-F, 5'-GCACCCATCCTCATCCAG-3', and E7-R, 5'-CTGAGTCGCTTTGTGGGT-3'. To validate the knockdown efficiency of aMO, the pCS2-UTR-*rnf31*-EGFP plasmid with aMO target sequence was coinjected with *rnf31*-aMOs or control-MOs into zebrafish embryos at the one-cell stage.

For the rescue experiments, zebrafish *rnf31*-aMO-resistant full-length mRNAs were transcribed from pCS2-aMO-resistant *rnf31* plasmids using the mMESSAGE mMACHINE SP6 Kit (Thermo Fisher Scientific) and together injected with *rnf31*-aMOs into zebrafish embryos at the one-cell stage. For whole-mount in situ hybridization, the control or *rnf31*-knockdown embryos were fixed in 4% PFA and hybridized with digoxigenin-labeled *cm1c2* probes at 65°C. This study was approved by Shanghai Institutes for Biological Sciences, Chinese Academy of Sciences.

### Statistical analysis

Statistical calculations were performed with SPSS software (IBM Corp.). The normality of all data were performed by the Shapiro–Wilk test, and the homogeneity of variance was performed by Levene's test. An unpaired two-tailed *t* test was applied for statistical comparisons between two groups that conform to normal distribution. Multiple comparisons were tested by one-way ANOVA followed by Bonferroni's or Dunnett's multiple comparison test, as noted in the figure legends. For all tests, differences were considered statistically significant if  $P < 0.05$  (\*,  $P < 0.05$ ; \*\*,  $P < 0.01$ ; \*\*\*,  $P < 0.001$ ). No statistical methods were used to predetermine sample size. The experiments were not randomized. No samples were excluded. The investigators were blinded for assessment of all the staining assays.

### Online supplemental material

Fig. S1 shows that LUBAC is essential for ciliogenesis in mIMCD-3 cells and left–right asymmetry in zebrafish. Fig. S2 shows that loss of LUBAC does not affect centrosome structure and TZ assembly. Fig. S3 illustrates that LUBAC and the linear ubiquitin chains localized at the centrosome. Fig. S4 maps the region of CP110 interacting with HOIP and shows that OTULIN inhibits CP110 removal and ciliogenesis. Fig. S5 illustrates that PRPF8 is identified as the receptor of linear ubiquitin chains by LC-MS/MS. Fig. S6 shows that PRPF8 localizes at the mother centriole in RPE-1 cells. Fig. S7 shows that the functional impairment of PRPF8 in pre-mRNA splicing does not affect ciliogenesis. Table S1 shows the bound proteins of linear ubiquitin chains identified by MS.

### Data availability

The data that support the findings of this study are available from the corresponding author upon reasonable request.

## Acknowledgments

We thank Prof. Xue-liang Zhu, Vishva M. Dixit, and Brian David Dynlacht for providing cells, antibodies, and plasmids.

This work was funded by the National Basic Research Program of China (2014CB910603), National Natural Science Foundation of China (81521064, 81790252, 82002970), and National Key Research and Development Program (2017YFC1601100, 2017YFC1601101, 2017YFC1601102, 2017YFC1601104, 2017YFA0503900).

The authors declare no competing financial interests.

Author contributions: H.-Y. Li, N. Wang, and Y.-C. Zhang supervised the project; X.-L. Shen and J.-F. Yuan designed and carried out most of the experiments; X.-H. Qin, Y.-L. Xu, H.-Q. Tu, Z.-Q. Song, P.-Y. Li, H.-B. Hu, S. Li, Q. Han, and M. Wu provided reagents and suggestions; X.-X. Jian, J.-N. Li, C.-Y. He, K. Wang, L.-Y. Liang, X.-P. Yu, and G.-P. Song analyzed the data; T. Zhou and A.-L. Li carried out the statistics; and X.-L. Shen, J.-F. Yuan, Y.-C. Zhang, H.-Y. Li, and N. Wang wrote the paper. All authors discussed the results and commented on the manuscript.

Submitted: 16 May 2021

Revised: 13 September 2021

Accepted: 15 October 2021

## References

- Badano, J.L., N. Mitsuma, P.L. Beales, and N. Katsanis. 2006. The ciliopathies: an emerging class of human genetic disorders. *Annu Rev Genomics Hum Genet.* 7:125–148.
- Bergmann, C., L.M. Guay-Woodford, P.C. Harris, S. Horie, D.J.M. Peters, V.E. Torres. 2018. Polycystic kidney disease. *Nat Rev Dis Primers.* 4:50.
- Bettencourt-Dias, M., and Z. Carvalho-Santos. 2008. Double life of centrioles: CP110 in the spotlight. *Trends Cell Biol.* 18:8–11. <https://doi.org/10.1016/j.tcb.2007.11.002>
- Brown, J.D., and J.D. Beggs. 1992. Roles of PRP8 protein in the assembly of splicing complexes. *EMBO J.* 11:3721–3729. <https://doi.org/10.1002/j.1460-2075.1992.tb05457.x>
- Capdevila, J., K.J. Vogan, C.J. Tabin, and J.C. Izpisua Belmonte. 2000. Mechanisms of left-right determination in vertebrates. *Cell.* 101:9–21. [https://doi.org/10.1016/S0092-8674\(00\)80619-4](https://doi.org/10.1016/S0092-8674(00)80619-4)
- Chattopadhyay, S., T. Kuzmanovic, Y. Zhang, J.L. Wetzel, and G.C. Sen. 2016. Ubiquitination of the transcription factor IRF-3 activates RIPA, the apoptotic pathway that protects mice from viral pathogenesis. *Immunity.* 44:1151–1161. <https://doi.org/10.1016/j.immuni.2016.04.009>
- Corbit, K.C., A.E. Shyer, W.E. Dowdle, J. Gauden, V. Singla, M.H. Chen, P.T. Chuang, and J.F. Reiter. 2008. Kif3a constrains beta-catenin-dependent Wnt signalling through dual ciliary and non-ciliary mechanisms. *Nat. Cell Biol.* 10:70–76. <https://doi.org/10.1038/ncb1670>
- Emmerich, C.H., A. Ordureau, S. Strickson, J.S. Arthur, P.G. Pedrioli, D. Komander, and P. Cohen. 2013. Activation of the canonical IKK complex by K63/M1-linked hybrid ubiquitin chains. *Proc. Natl. Acad. Sci. USA.* 110:15247–15252. <https://doi.org/10.1073/pnas.1314715110>
- Essner, J.J., J.D. Amack, M.K. Nyholm, E.B. Harris, and H.J. Yost. 2005. Kupffer's vesicle is a ciliated organ of asymmetry in the zebrafish embryo that initiates left-right development of the brain, heart and gut. *Development.* 132:1247–1260. <https://doi.org/10.1242/dev.01663>
- Farkas, M.H., D.S. Lew, M.E. Sousa, K. Bujakowska, J. Chatagnon, S.S. Bhat-tacharya, E.A. Pierce, and E.F. Nandrot. 2014. Mutations in pre-mRNA processing factors 3, 8, and 31 cause dysfunction of the retinal pigment epithelium. *Am. J. Pathol.* 184:2641–2652. <https://doi.org/10.1016/j.ajpath.2014.06.026>
- French, M.E., C.F. Koehler, and T. Hunter. 2021. Emerging functions of branched ubiquitin chains. *Cell Discov.* 7:6. <https://doi.org/10.1038/s41421-020-00237-y>
- Fu, Y., H. Wang, H. Dai, Q. Zhu, C.P. Cui, X. Sun, Y. Li, Z. Deng, X. Zhou, Y. Ge, et al. 2021. OTULIN allies with LUBAC to govern angiogenesis by editing

- ALK1 linear polyubiquitin. *Mol. Cell.* 81:3187–3204.e7. <https://doi.org/10.1016/j.molcel.2021.05.031>
- Garcia-Gonzalo, F.R., K.C. Corbit, M.S. Sirerol-Piquer, G. Ramaswami, E.A. Otto, T.R. Noriega, A.D. Seol, J.F. Robinson, C.L. Bennett, D.J. Josifova, et al. 2011. A transition zone complex regulates mammalian ciliogenesis and ciliary membrane composition. *Nat. Genet.* 43:776–784. <https://doi.org/10.1038/ng.891>
- Gerdes, J.M., E.E. Davis, and N. Katsanis. 2009. The vertebrate primary cilium in development, homeostasis, and disease. *Cell.* 137:32–45. <https://doi.org/10.1016/j.cell.2009.03.023>
- Gerlach, B., S.M. Cordier, A.C. Schmukle, C.H. Emmerich, E. Rieser, T.L. Haas, A.I. Webb, J.A. Rickard, H. Anderton, W.W. Wong, et al. 2011. Linear ubiquitination prevents inflammation and regulates immune signaling. *Nature.* 471:591–596. <https://doi.org/10.1038/nature09816>
- Goetz, S.C., K.F. Liem Jr., and K.V. Anderson. 2012. The spinocerebellar ataxia-associated gene Tau tubulin kinase 2 controls the initiation of ciliogenesis. *Cell.* 151:847–858. <https://doi.org/10.1016/j.cell.2012.10.010>
- Gonçalves, A.B., S.K. Hasselbalch, B.B. Joensen, S. Patzke, P. Martens, S.K. Ohlsen, M. Quinodoz, K. Nikopoulos, R. Suleiman, M.P. Damsø Jeppesen, et al. 2021. CEP78 functions downstream of CEP350 to control biogenesis of primary cilia by negatively regulating CP110 levels. *eLife.* 10: e63731.
- Grainger, R.J., and J.D. Beggs. 2005. Prp8 protein: at the heart of the spliceosome. *RNA.* 11:533–557. <https://doi.org/10.1261/rna.2220705>
- Haglund, K., and I. Dikic. 2005. Ubiquitylation and cell signaling. *EMBO J.* 24:3353–3359. <https://doi.org/10.1038/sj.emboj.7600808>
- Hong, H., J. Kim, and J. Kim. 2015. Myosin heavy chain 10 (MYH10) is required for centriole migration during the biogenesis of primary cilia. *Biochem. Biophys. Res. Commun.* 461:180–185. <https://doi.org/10.1016/j.bbrc.2015.04.028>
- Hossain, D., Y. Javadi Esfehiani, A. Das, and W.Y. Tsang. 2017. Cep78 controls centrosome homeostasis by inhibiting EDD-DYRK2-DDB1<sup>VPrBP</sup>. *EMBO Rep.* 18:632–644. <https://doi.org/10.15252/embr.201642377>
- Hu, H.B., Z.Q. Song, G.P. Song, S. Li, H.Q. Tu, M. Wu, Y.C. Zhang, J.F. Yuan, T.T. Li, P.Y. Li, et al. 2021. LPA signaling acts as a cell-extrinsic mechanism to initiate cilia disassembly and promote neurogenesis. *Nat. Commun.* 12:662. <https://doi.org/10.1038/s41467-021-20986-y>
- Huang, N., D. Zhang, F. Li, P. Chai, S. Wang, J. Teng, and J. Chen. 2018. M-phase phosphoprotein 9 regulates ciliogenesis by modulating CP110-CEP97 complex localization at the mother centriole. *Nat. Commun.* 9:4511. <https://doi.org/10.1038/s41467-018-06990-9>
- Ikeda, F. 2015. Linear ubiquitination signals in adaptive immune responses. *Immunol. Rev.* 266:222–236. <https://doi.org/10.1111/imr.12300>
- Ikeda, F., and I. Dikic. 2008. Atypical ubiquitin chains: new molecular signals. 'Protein Modifications: Beyond the Usual Suspects' review series. *EMBO Rep.* 9:536–542. <https://doi.org/10.1038/embor.2008.93>
- Iwai, K., and F. Tokunaga. 2009. Linear polyubiquitination: a new regulator of NF-kappaB activation. *EMBO Rep.* 10:706–713. <https://doi.org/10.1038/embor.2009.144>
- Iwai, K., H. Fujita, and Y. Sasaki. 2014. Linear ubiquitin chains: NF-κB signalling, cell death and beyond. *Nat. Rev. Mol. Cell Biol.* 15:503–508. <https://doi.org/10.1038/nrm3836>
- Joo, K., C.G. Kim, M.S. Lee, H.Y. Moon, S.H. Lee, M.J. Kim, H.S. Kweon, W.Y. Park, C.H. Kim, J.G. Gleeson, and J. Kim. 2013. CCDC41 is required for ciliary vesicle docking to the mother centriole. *Proc. Natl. Acad. Sci. USA.* 110:5987–5992. <https://doi.org/10.1073/pnas.1220927110>
- Juan, T., C. Géminard, J.B. Coutelis, D. Cerezo, S. Polès, S. Noselli, and M. Fürthauer. 2018. Myosin1D is an evolutionarily conserved regulator of animal left-right asymmetry. *Nat. Commun.* 9:1942. <https://doi.org/10.1038/s41467-018-04284-8>
- Keusekotten, K., P.R. Elliott, L. Glockner, B.K. Fiil, R.B. Damgaard, Y. Kulathu, T. Wauer, M.K. Hospenthal, M. Gyrd-Hansen, D. Krappmann, et al. 2013. OTULIN antagonizes LUBAC signaling by specifically hydrolyzing Met1-linked polyubiquitin. *Cell.* 153:1312–1326. <https://doi.org/10.1016/j.cell.2013.05.014>
- Kim, S., and B.D. Dynlacht. 2013. Assembling a primary cilium. *Curr. Opin. Cell Biol.* 25:506–511. <https://doi.org/10.1016/j.cob.2013.04.011>
- Kirisako, T., K. Kamei, S. Murata, M. Kato, H. Fukumoto, M. Kanie, S. Sano, F. Tokunaga, K. Tanaka, and K. Iwai. 2006. A ubiquitin ligase complex assembles linear polyubiquitin chains. *EMBO J.* 25:4877–4887. <https://doi.org/10.1038/sj.emboj.7601360>
- Kobayashi, T., W.Y. Tsang, J. Li, W. Lane, and B.D. Dynlacht. 2011. Centriolar kinesin Kif24 interacts with CP110 to remodel microtubules and regulate ciliogenesis. *Cell.* 145:914–925. <https://doi.org/10.1016/j.cell.2011.04.028>

- Komander, D., and M. Rape. 2012. The ubiquitin code. *Annu. Rev. Biochem.* 81: 203–229. <https://doi.org/10.1146/annurev-biochem-060310-170328>
- Kuhns, S., K.N. Schmidt, J. Reymann, D.F. Gilbert, A. Neuner, B. Hub, R. Carvalho, P. Wiedemann, H. Zentgraf, H. Erfle, et al. 2013. The microtubule affinity regulating kinase MARK4 promotes axoneme extension during early ciliogenesis. *J. Cell Biol.* 200:505–522. <https://doi.org/10.1083/jcb.201206013>
- Lafont, E., P. Draber, E. Rieser, M. Reichert, S. Kupka, D. de Miguel, H. Draberova, A. von Mässenhausen, A. Bhamra, S. Henderson, et al. 2018. TBK1 and IKKε prevent TNF-induced cell death by RIPK1 phosphorylation. *Nat. Cell Biol.* 20:1389–1399. <https://doi.org/10.1038/s41556-018-0229-6>
- Li, J., S. Kim, T. Kobayashi, F.X. Liang, N. Korzeniewski, S. Duensing, and B.D. Dynlacht. 2012. Neurl4, a novel daughter centriole protein, prevents formation of ectopic microtubule organizing centres. *EMBO Rep.* 13: 547–553. <https://doi.org/10.1038/embor.2012.40>
- Long, S., N. Ahmad, and M. Rebagliati. 2003. The zebrafish nodal-related gene southpaw is required for visceral and diencephalic left-right asymmetry. *Development.* 130:2303–2316. <https://doi.org/10.1242/dev.00436>
- Loukil, A., K. Tormanen, and C. Sütterlin. 2017. The daughter centriole controls ciliogenesis by regulating Neurl-4 localization at the centrosome. *J. Cell Biol.* 216:1287–1300. <https://doi.org/10.1083/jcb.201608119>
- Malinová, A., Z. Cvačková, D. Matějů, Z. Hořejší, C. Abéza, F. Vandermoere, E. Bertrand, D. Staněk, and C. Verheggen. 2017. Assembly of the U5 snRNP component PRPF8 is controlled by the HSP90/R2TP chaperones. *J. Cell Biol.* 216:1579–1596. <https://doi.org/10.1083/jcb.201701165>
- Matsumoto, M.L., K.C. Dong, C. Yu, L. Phu, X. Gao, R.N. Hannoush, S.G. Hymowitz, D.S. Kirkpatrick, V.M. Dixit, and R.F. Kelley. 2012. Engineering and structural characterization of a linear polyubiquitin-specific antibody. *J. Mol. Biol.* 418:134–144. <https://doi.org/10.1016/j.jmb.2011.12.053>
- McKie, A.B., J.C. McHale, T.J. Keen, E.E. Tarttelin, R. Goliath, J.J. van Lith-Verhoeven, J. Greenberg, R.S. Ramesar, C.B. Hoyng, F.P. Cremers, et al. 2001. Mutations in the pre-mRNA splicing factor gene PRPC8 in autosomal dominant retinitis pigmentosa (RP13). *Hum. Mol. Genet.* 10: 1555–1562. <https://doi.org/10.1093/hmg/10.15.1555>
- Nagai, T., S. Mukoyama, H. Kagiwada, N. Goshima, and K. Mizuno. 2018. Cullin-3-KCTD10-mediated CEP97 degradation promotes primary cilium formation. *J. Cell Sci.* 131:jcs.219527. <https://doi.org/10.1242/jcs.219527>
- Nigg, E.A., and J.W. Raff. 2009. Centrioles, centrosomes, and cilia in health and disease. *Cell.* 139:663–678. <https://doi.org/10.1016/j.cell.2009.10.036>
- Pazour, G.J., J.T. San Agustin, J.A. Follit, J.L. Rosenbaum, and G.B. Witman. 2002. Polycystin-2 localizes to kidney cilia and the ciliary level is elevated in orpk mice with polycystic kidney disease. *Curr. Biol.* 12: R378–R380. [https://doi.org/10.1016/S0960-9822\(02\)00877-1](https://doi.org/10.1016/S0960-9822(02)00877-1)
- Peltzer, N., E. Rieser, L. Taraborrelli, P. Draber, M. Darding, B. Pernaute, Y. Shimizu, A. Sarr, H. Draberova, A. Montinaro, et al. 2014. HOIP deficiency causes embryonic lethality by aberrant TNFR1-mediated endothelial cell death. *Cell Rep.* 9:153–165. <https://doi.org/10.1016/j.celrep.2014.08.066>
- Peltzer, N., M. Darding, A. Montinaro, P. Draber, H. Draberova, S. Kupka, E. Rieser, A. Fisher, C. Hutchinson, L. Taraborrelli, et al. 2018. LUBAC is essential for embryogenesis by preventing cell death and enabling haematopoiesis. *Nature.* 557:112–117. <https://doi.org/10.1038/s41586-018-0064-8>
- Pena, V., S. Liu, J.M. Bujnicki, R. Lührmann, and M.C. Wahl. 2007. Structure of a multipartite protein-protein interaction domain in splicing factor prp8 and its link to retinitis pigmentosa. *Mol. Cell.* 25:615–624. <https://doi.org/10.1016/j.molcel.2007.01.023>
- Prosser, S.L., and C.G. Morrison. 2015. Centrin2 regulates CP110 removal in primary cilium formation. *J. Cell Biol.* 208:693–701. <https://doi.org/10.1083/jcb.201411070>
- Rahighi, S., F. Ikeda, M. Kawasaki, M. Akutsu, N. Suzuki, R. Kato, T. Kensche, T. Uejima, S. Bloor, D. Komander, et al. 2009. Specific recognition of linear ubiquitin chains by NEMO is important for NF-κappaB activation. *Cell.* 136:1098–1109. <https://doi.org/10.1016/j.cell.2009.03.007>
- Rivkin, E., S.M. Almeida, D.F. Ceccarelli, Y.C. Juang, T.A. MacLean, T. Sri-kumar, H. Huang, W.H. Dunham, R. Fukumura, G. Xie, et al. 2013. The linear ubiquitin-specific deubiquitinase gumbly regulates angiogenesis. *Nature.* 498:318–324. <https://doi.org/10.1038/nature12296>
- Rodgers, M.A., J.W. Bowman, H. Fujita, N. Orazio, M. Shi, Q. Liang, R. Amaty, T.J. Kelly, K. Iwai, J. Ting, and J.U. Jung. 2014. The linear ubiquitin assembly complex (LUBAC) is essential for NLRP3 inflammasome activation. *J. Exp. Med.* 211:1333–1347. <https://doi.org/10.1084/jem.20132486>
- Rohatgi, R., L. Milenkovic, and M.P. Scott. 2007. Patched1 regulates hedgehog signaling at the primary cilium. *Science.* 317:372–376. <https://doi.org/10.1126/science.1139740>
- Sánchez, I., and B.D. Dynlacht. 2016. Cilium assembly and disassembly. *Nat. Cell Biol.* 18:711–717. <https://doi.org/10.1038/ncb3370>
- Sang, L., J.J. Miller, K.C. Corbit, R.H. Giles, M.J. Brauer, E.A. Otto, L.M. Baye, X. Wen, S.J. Scales, M. Kwong, et al. 2011. Mapping the NPHP-JBTS-MKS protein network reveals ciliopathy disease genes and pathways. *Cell.* 145:513–528. <https://doi.org/10.1016/j.cell.2011.04.019>
- Shearer, R.F., K.M. Frikstad, J. McKenna, R.A. McCloy, N. Deng, A. Burgess, T. Stokke, S. Patzke, and D.N. Saunders. 2018. The E3 ubiquitin ligase UBR5 regulates centriolar satellite stability and primary cilia. *Mol. Biol. Cell.* 29:1542–1554. <https://doi.org/10.1091/mbc.E17-04-0248>
- Singla, V., and J.F. Reiter. 2006. The primary cilium as the cell's antenna: signaling at a sensory organelle. *Science.* 313:629–633. <https://doi.org/10.1126/science.1124534>
- Smit, J.J., D. Monteferrario, S.M. Noordermeer, W.J. van Dijk, B.A. van der Reijden, and T.K. Sixma. 2012. The E3 ligase HOIP specifies linear ubiquitin chain assembly through its RING-IBR-RING domain and the unique LDD extension. *EMBO J.* 31:3833–3844. <https://doi.org/10.1038/emboj.2012.217>
- Song, E.J., S.L. Werner, J. Neubauer, F. Stegmeier, J. Aspden, D. Rio, J.W. Harper, S.J. Elledge, M.W. Kirschner, and M. Rape. 2010. The Prp19 complex and the Usp4Sart3 deubiquitinating enzyme control reversible ubiquitination at the spliceosome. *Genes Dev.* 24:1434–1447. <https://doi.org/10.1101/gad.1925010>
- Spektor, A., W.Y. Tsang, D. Khoo, and B.D. Dynlacht. 2007. Cep97 and CP110 suppress a cilia assembly program. *Cell.* 130:678–690. <https://doi.org/10.1016/j.cell.2007.06.027>
- Stainier, D.Y.R., E. Raz, N.D. Lawson, S.C. Ekker, R.D. Burdine, J.S. Eisen, P.W. Ingham, S. Schulte-Merker, D. Yelon, B.M. Weinstein, et al. 2017. Guidelines for morpholino use in zebrafish. *PLoS Genet.* 13:e1007000. <https://doi.org/10.1371/journal.pgen.1007000>
- Stieglitz, B., A.C. Morris-Davies, M.G. Koliopoulos, E. Christodoulou, and K. Rittinger. 2012. LUBAC synthesizes linear ubiquitin chains via a thioester intermediate. *EMBO Rep.* 13:840–846. <https://doi.org/10.1038/embor.2012.105>
- Tokunaga, F., S. Sakata, Y. Saeki, Y. Satomi, T. Kirisako, K. Kamei, T. Nakagawa, M. Kato, S. Murata, S. Yamaoka, et al. 2009. Involvement of linear polyubiquitylation of NEMO in NF-κappaB activation. *Nat. Cell Biol.* 11:123–132. <https://doi.org/10.1038/ncb1821>
- Tsang, W.Y., C. Bossard, H. Khanna, J. Peränen, A. Swaroop, V. Malhotra, and B.D. Dynlacht. 2008. CP110 suppresses primary cilia formation through its interaction with CEP290, a protein deficient in human ciliary disease. *Dev. Cell.* 15:187–197. <https://doi.org/10.1016/j.devcel.2008.07.004>
- Tu, H.Q., X.H. Qin, Z.B. Liu, Z.Q. Song, H.B. Hu, Y.C. Zhang, Y. Chang, M. Wu, Y. Huang, Y.F. Bai, et al. 2018. Microtubule asters anchored by FSD1 control axoneme assembly and ciliogenesis. *Nat. Commun.* 9:5277. <https://doi.org/10.1038/s41467-018-07664-2>
- Valente, E.M., C.V. Logan, S. Mougou-Zerelli, J.H. Lee, J.L. Silhavy, F. Brancati, M. Iannicelli, L. Travaglini, S. Romani, B. Illi, et al. 2010. Mutations in TMEM216 perturb ciliogenesis and cause Joubert, Meckel and related syndromes. *Nat. Genet.* 42:619–625. <https://doi.org/10.1038/ng.594>
- Varshavsky, A. 2017. The ubiquitin system, autophagy, and regulated protein degradation. *Annu. Rev. Biochem.* 86:123–128. <https://doi.org/10.1146/annurev-biochem-061516-044859>
- Wang, G., H.B. Hu, Y. Chang, Y. Huang, Z.Q. Song, S.B. Zhou, L. Chen, Y.C. Zhang, M. Wu, H.Q. Tu, et al. 2019. Rab7 regulates primary cilia disassembly through cilia excision. *J. Cell Biol.* 218:4030–4041. <https://doi.org/10.1083/jcb.201811136>
- Whewey, G., M. Schmidts, D.A. Mans, K. Szymanska, T.T. Nguyen, H. Racher, I.G. Phelps, G. Toedt, J. Kennedy, K.A. Wunderlich, et al. 2015. An siRNA-based functional genomics screen for the identification of regulators of ciliogenesis and ciliopathy genes. *Nat. Cell Biol.* 17:1074–1087. <https://doi.org/10.1038/ncb3201>
- Williams, C.L., C. Li, K. Kida, P.N. Inglis, S. Mohan, L. Semencik, N.J. Bialas, R.M. Stupay, N. Chen, O.E. Blacque, et al. 2011. MKS and NPHP modules cooperate to establish basal body/transition zone membrane associations and ciliary gate function during ciliogenesis. *J. Cell Biol.* 192: 1023–1041. <https://doi.org/10.1083/jcb.201012116>
- Wong, S.Y., A.D. Seol, P.L. So, A.N. Ermilov, C.K. Bichakjian, E.H. Epstein Jr., A.A. Dlugosz, and J.F. Reiter. 2009. Primary cilia can both mediate and



- suppress hedgehog pathway-dependent tumorigenesis. *Nat. Med.* 15: 1055–1061. <https://doi.org/10.1038/nm.2011>
- Wu, C.T., H.Y. Chen, and T.K. Tang. 2018. Myosin-Va is required for preciliary vesicle transportation to the mother centriole during ciliogenesis. *Nat. Cell Biol.* 20:175–185. <https://doi.org/10.1038/s41556-017-0018-7>
- Wu, M., Y. Chang, H. Hu, R. Mu, Y. Zhang, X. Qin, X. Duan, W. Li, H. Tu, W. Zhang, et al. 2019. LUBAC controls chromosome alignment by targeting CENP-E to attached kinetochores. *Nat. Commun.* 10:273. <https://doi.org/10.1038/s41467-018-08043-7>
- Yadav, S.P., N.K. Sharma, C. Liu, L. Dong, T. Li, and A. Swaroop. 2016. Centrosomal protein CP110 controls maturation of the mother centriole during cilia biogenesis. *Development.* 143:1491–1501.
- Yau, R., and M. Rape. 2016. The increasing complexity of the ubiquitin code. *Nat. Cell Biol.* 18:579–586. <https://doi.org/10.1038/ncb3358>
- Yelon, D., S.A. Horne, and D.Y. Stainier. 1999. Restricted expression of cardiac myosin genes reveals regulated aspects of heart tube assembly in zebrafish. *Dev. Biol.* 214:23–37. <https://doi.org/10.1006/dbio.1999.9406>
- Zaghloul, N.A., and N. Katsanis. 2009. Mechanistic insights into Bardet-Biedl syndrome, a model ciliopathy. *J. Clin. Invest.* 119:428–437. <https://doi.org/10.1172/JCI37041>
- Zhang, Y.C., Y.F. Bai, J.F. Yuan, X.L. Shen, Y.L. Xu, X.X. Jian, S. Li, Z.Q. Song, H.B. Hu, P.Y. Li, et al. 2021. CEP55 promotes cilia disassembly through stabilizing Aurora A kinase. *J. Cell Biol.* 220:e202003149.
- Zuo, Y., Q. Feng, L. Jin, F. Huang, Y. Miao, J. Liu, Y. Xu, X. Chen, H. Zhang, T. Guo, et al. 2020. Regulation of the linear ubiquitination of STAT1 controls antiviral interferon signaling. *Nat. Commun.* 11:1146. <https://doi.org/10.1038/s41467-020-14948-z>

## Supplemental material

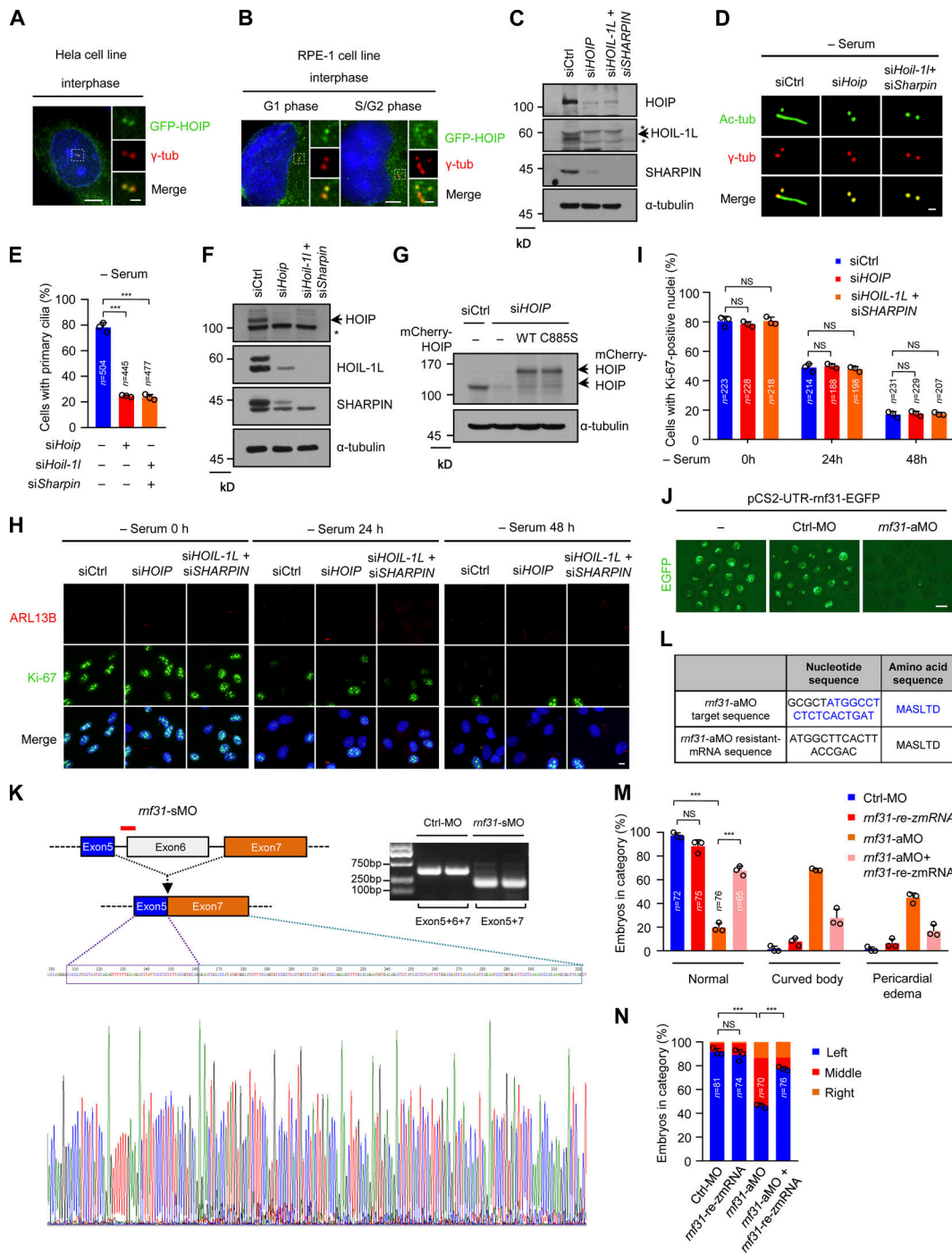


Figure S1. **LUBAC is essential for ciliogenesis in mIMCD-3 cells and left-right asymmetry in zebrafish (related to Fig. 1).** (A and B) HOIP was localized at the centrosome in interphase cells. HeLa cells (A) or RPE-1 cells (B) were transfected with GFP-HOIP and then stained with  $\gamma$ -tubulin ( $\gamma$ -tub, red). Insets show zoomed-in views of the boxed regions. Scale bars, 5  $\mu$ m (main image) and 1  $\mu$ m (magnified region). (C) RPE-1 cell lysates in Fig. 1 A were analyzed by immunoblotting with the indicated antibodies. (D) mIMCD-3 cells were transfected with control or LUBAC component siRNAs and serum starved for 48 h. The cells were stained with indicated antibodies. Scale bar, 1  $\mu$ m. Ac-tubulin (Ac-tub) is a ciliary marker. (E) Quantification of the ciliated cells in D. (F) The knockdown efficiency of LUBAC in mIMCD-3 cells was analyzed by immunoblotting with the indicated antibodies. (G) RPE-1 cell lysates in Fig. 1 C were analyzed by immunoblotting with the indicated antibodies. (H) RPE-1 cells were transfected with control or LUBAC component siRNAs followed by serum starving for the indicated time points, and then the cells were stained with Ki-67, ARL13B, and Hoechst (DNA, blue). Scale bar, 10  $\mu$ m. (I) Quantification of Ki-67-positive cells in H at the indicated time points. (J) The knockdown efficiency of *mf31*-aMO was validated by the EGFP intensity expressed from the pCS2-UTR-*mf31*-EGFP plasmid with aMO target sequence. Scale bar, 1 mm. (K) The knockdown efficiency of *mf31*-sMO was analyzed by sequencing and RT-PCR. (L) The target sequence of *mf31*-aMO and sequence of *mf31*-rezmRNA. (M) The injection of *mf31*-rezmRNA rescued curved body and pericardial edema in *mf31*-aMO knockdown morphants. (N) The expression of *mf31*-rezmRNA rescued the defective left-right asymmetry in *mf31*-aMO knockdown morphants. Data are presented as mean  $\pm$  SD of three independent experiments in E, I, M, and N. \*\*\*,  $P < 0.001$  by one-way ANOVA with Dunnett's multiple comparisons test in E and Bonferroni's multiple comparisons test in M and N. The asterisks in C and F indicate nonspecific bands. Ctrl, control.

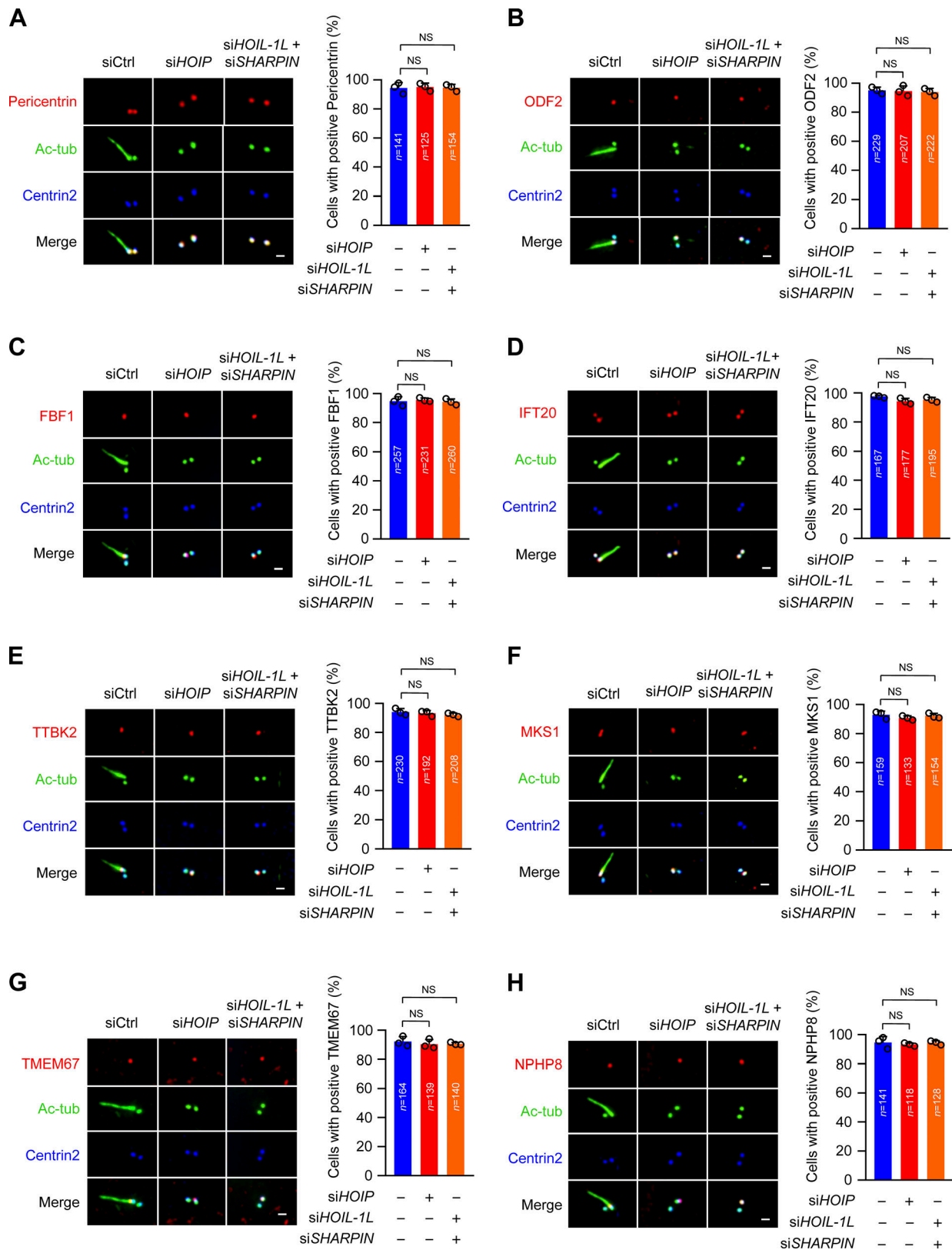


Figure S2. **Loss of LUBAC does not affect centrosome structure and TZ assembly (related to Fig. 2).** (A–H) RPE-1 cells were transfected with control or LUBAC component siRNAs and serum starved for 48 h. The cells were stained with the indicated antibodies. Scale bars, 1  $\mu$ m. (A) The localization of pericentrin was normal in LUBAC-depleted RPE-1 cells. (B and C) The localization of subdistal appendage proteins ODF2 and FBF1 were not affected by LUBAC depletion. (D) The localization of IFT20 on the centrosome appeared normal in LUBAC-depleted cells. (E) LUBAC is not essential for the recruitment of TTBK2 to the mother centriole. (F–H) Depletion of LUBAC could not affect the localization of TZ proteins MKS1, TMEM67, and NPHP8. Data are presented as mean  $\pm$  SD of three independent experiments. Significance tested by one-way ANOVA with Dunnett’s multiple comparisons. Ctrl, control; tub, tubulin.

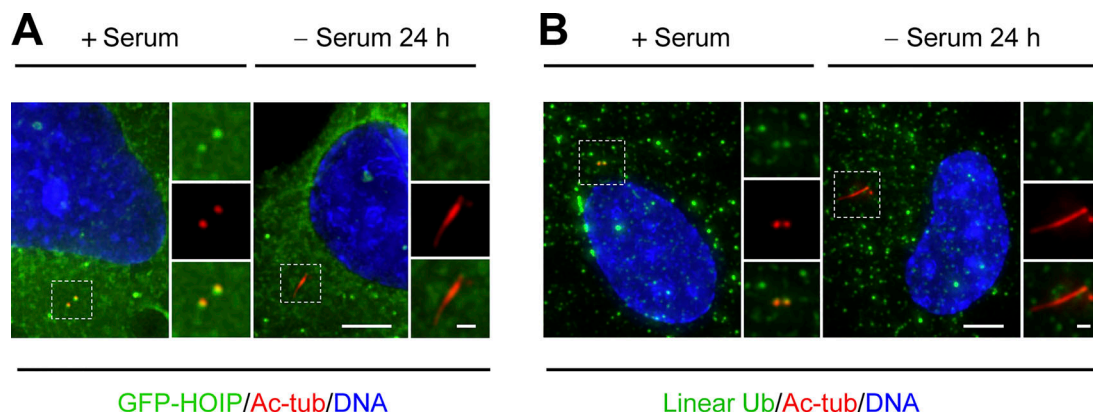


Figure S3. **LUBAC and the linear ubiquitin chains were localized at the centrosome (related to Fig. 3).** (A and B) RPE-1 cells were transfected with LUBAC components and cultured in the presence of serum or serum starved for 24 h. (A) The cells were stained with Ac-tubulin (Ac-tub). Insets show zoomed-in views of the boxed regions. Scale bars, 5  $\mu\text{m}$  (main image) and 1  $\mu\text{m}$  (magnified region). (B) The cells stained with Ac-tub ( ) and anti-linear ubiquitin (Ub). Insets show zoomed-in views of the boxed regions. Scale bars, 5  $\mu\text{m}$  (main image) and 1  $\mu\text{m}$  (magnified region).

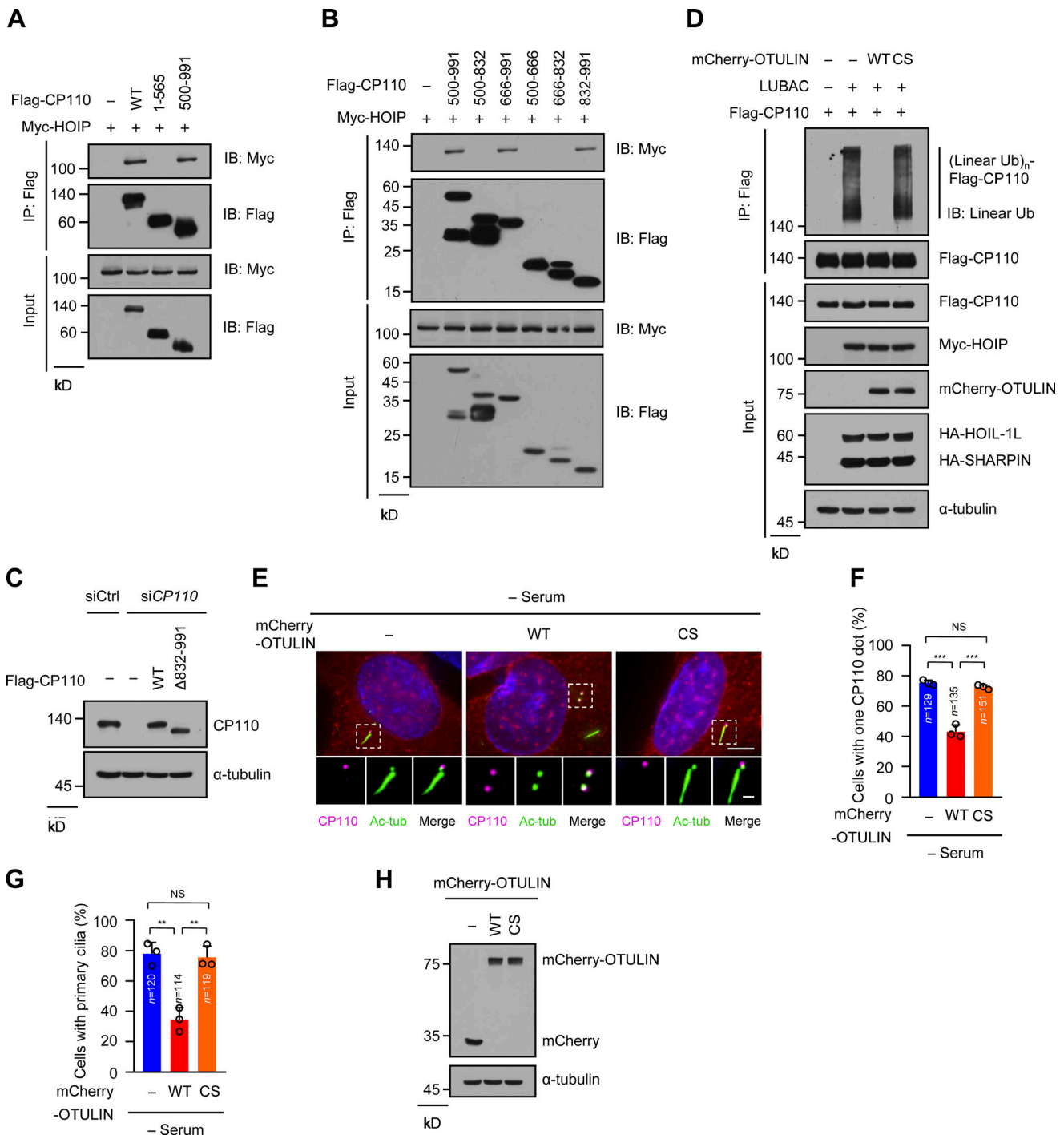


Figure S4. **Map of the region of CP110 interacting with HOIP and OTULIN inhibition of CP110 removal and ciliogenesis (related to Fig. 4).** (A and B) HEK293T cells were transfected with Myc-HOIP together with Flag-vector (-), Flag-CP110 WT, or a series of Flag-CP110 truncations. The cell lysates were immunoprecipitated with ANTI-FLAG M2 Affinity Gel. The immunoprecipitates and cell lysates then were analyzed by immunoblotting with the indicated antibodies. (C) RPE-1 cell lysates in Fig. 4 D were analyzed by immunoblotting with the indicated antibodies. (D) HEK293T cells were transfected with Flag-CP110 and LUBAC components together with mCherry-OTULIN WT or CS mutant. The subsequent linear ubiquitination assay procedures were similar to Fig. 3 C. (E) RPE-1 cells were transfected with mCherry-vector (-), mCherry-OTULIN WT, or CS mutant, then serum starved for 48 h. The cells were stained with the indicated antibodies. Insets show zoomed-in views of the boxed regions. Scale bars, 5  $\mu$ m (main image) and 1  $\mu$ m (magnified region). (F) Quantification of cells with one CP110 dot in mCherry-positive cells in E. (G) Quantification of the ciliated cells in mCherry-positive cells in E. (H) RPE-1 cell lysates in E were analyzed by immunoblotting with indicated antibodies. Data are presented as mean  $\pm$  SD of three independent experiments in F and G. \*\*,  $P < 0.01$ ; \*\*\*,  $P < 0.001$  by one-way ANOVA with Bonferroni's multiple comparisons test. IB, immunoblot; IP, immunoprecipitation; tub, tubulin; Ub, ubiquitin; (Linear Ub)<sub>n</sub>, poly-linear ubiquitin chains.

**A**

Identified candidate receptors for the linear ubiquitin chains by LC-MS/MS

NO.	Gene ID	Gene symbol	Protein Description
1	10594	PRPF8	pre-mRNA-processing-splicing factor 8
2	51366	UBR5	E3 ubiquitin-protein ligase UBR5
3	1642	DDB1	DNA damage-binding protein 1
4	4628	MYH10	myosin-10 isoform 1

**B**

Identified peptides of PRPF8 by LC-MS/MS

Region(aa)	Protein peptides
9-33	GPGNPVPGPLAPLPDYMSEEKLEK
228-240	WQFTLPMMSTLYR
342-362	TEDPDLPAFYFDPLINPISHR
675-686	QRVESHFDLELR
677-686	VESHFDLELR
728-741	VPGLPTPIENMILR
838-845	LLILALER
1058-1086	ASEMAGPPQMPNDFLSFQDIATEAAHPIR
1164-1180	SVTTVQWENSFVSVYSK
1263-1275	WNTALIGLMTYFR
1321-1341	ELGGLGMLSMGHVLIPOSDLR
1371-1384	YIQPWESEFIDSQR
1472-1491	TDMIQALGGVEGILEHTLFLK
1660-1667	YWIDIQLR
1793-1813	TFEGNLTKPINGAIFIFNPR
1841-1850	TAE EVAALIR
1995-2023	NNVNVASLTQSEIRDILGMEISAPSQQR
2009-2023	DIILGMEISAPSQQR
2035-2045	EQSQLTATQTR
2087-2108	TNHIYVSSDDIKETGYTYILPK

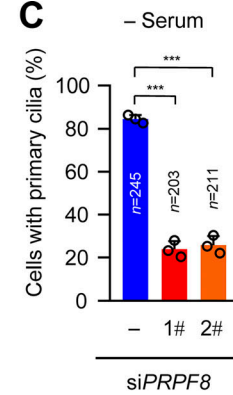
**C**


Figure S5. **PRPF8 is identified as the receptor of linear ubiquitin chains by LC-MS/MS (related to Fig. 5).** (A and B) The candidate proteins pulled down from the HEK293T cell lysates by GST-Ub4 were analyzed by LC-MS/MS. (A) A list of the candidate receptors of the linear ubiquitin chains. (B) A list of identified peptides of PRPF8 by LC-MS/MS in A. (C) Quantification of the ciliated cells in Fig. 5 C. Data are presented as mean  $\pm$  SD of three independent experiments. \*\*\*,  $P < 0.001$  by one-way ANOVA with Dunnett's multiple comparisons test. ID, identifier.

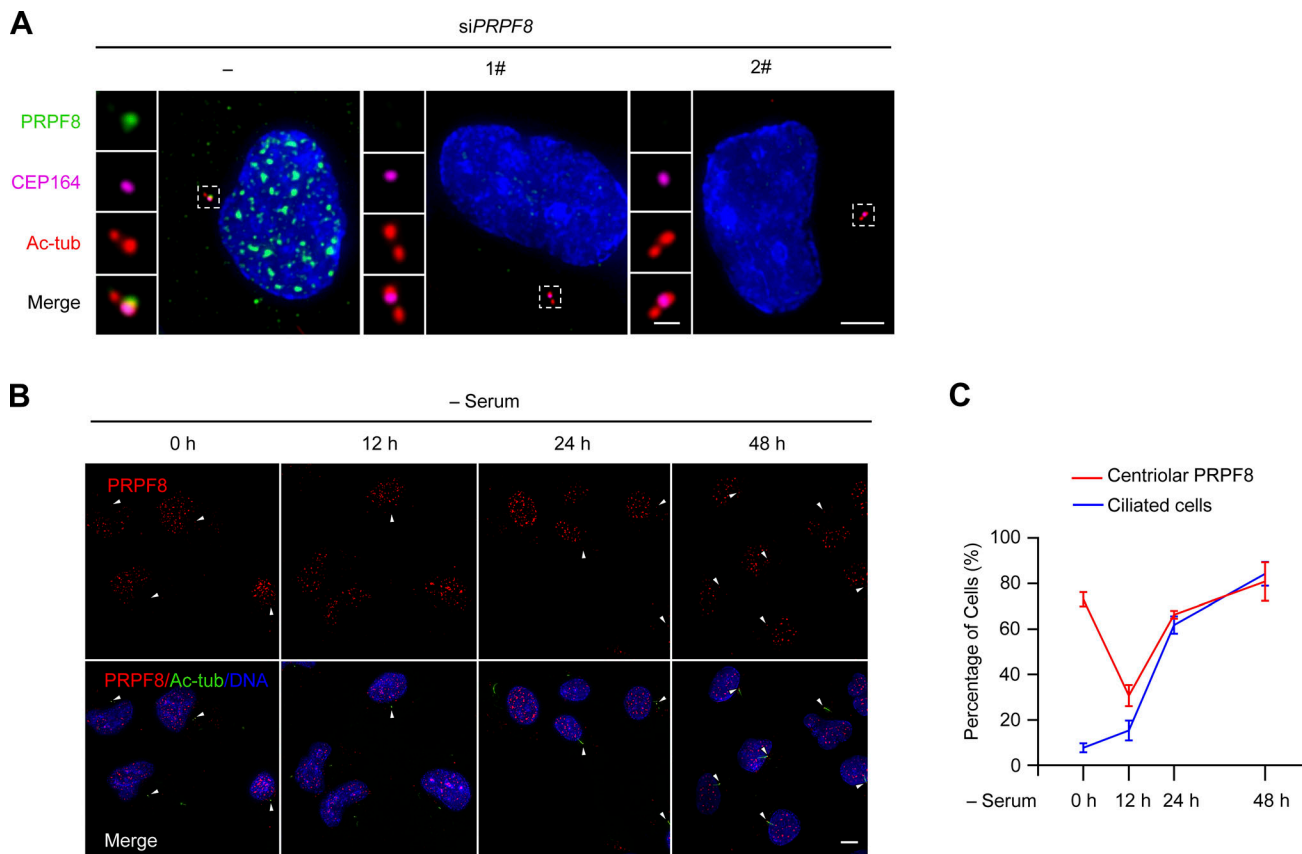


Figure S6. **PRPF8 localizes at the mother centriole in RPE-1 cells (related to Fig. 6).** **(A)** RPE-1 cells were transfected with control or PRPF8 siRNAs for 48 h. The cells were collected and stained with the indicated antibodies. Insets show zoomed-in views of the boxed regions. Scale bars, 5  $\mu$ m (main image) and 1  $\mu$ m (magnified region). PRPF8 (green) was localized at the mother centriole (marked by CEP164). **(B)** RPE-1 cells were serum starved for the indicated time points and stained with the indicated antibodies. White arrowheads indicate the centriolar PRPF8. Scale bar, 5  $\mu$ m. **(C)** Line graph showing the percentage of cells with primary cilia and centriolar PRPF8 in B. tub, tubulin.



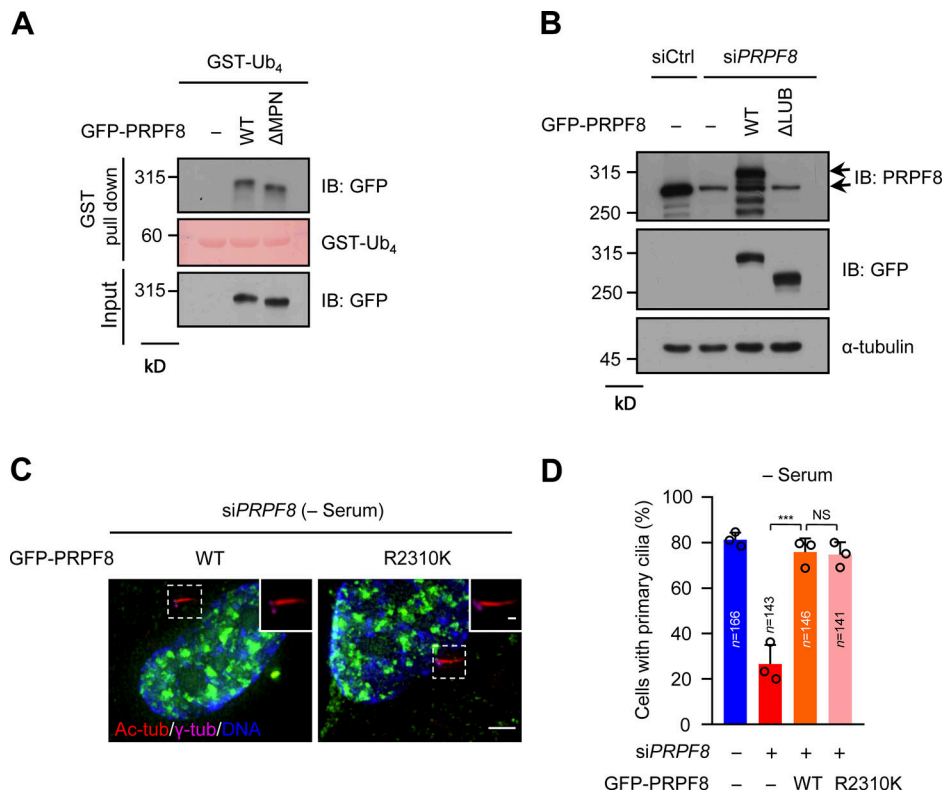


Figure S7. **The functional impairment of PRPF8 in pre-mRNA splicing does not affect ciliogenesis (related to Fig. 7).** (A) GFP-vector (-), GFP-PRPF8 WT, or ΔMPN mutant were transfected into HEK293T cells. The cell lysates were pulled down by GST-Ub4, and then GFP proteins were detected by anti-GFP antibody. GST-Ub4 was stained by Ponceau S. (B) RPE-1 cell lysates in Fig. 7 D were analyzed by immunoblotting with the indicated antibodies. (C) GFP-vector (-), GFP-PRPF8 WT, or GFP-PRPF8 R2310K mutant were transfected into control or PRPF8-depleted RPE-1 cells and serum starved for 48 h. The cells were stained with the indicated antibodies. Scale bars, 5 μm (main image) and 1 μm (magnified region). (D) Quantification of the ciliated cells in C. Data are presented as mean ± SD of three independent experiments. A one-way ANOVA test was performed followed by Bonferroni's multiple comparisons. \*\*\*, P < 0.001 by one-way ANOVA with Bonferroni's multiple comparisons test. IB, immunoblot; tub, tubulin.

Table S1, provided online as a separate Excel file, shows the bound proteins of linear ubiquitin chains identified by MS.